

RIGA TECHNICAL UNIVERSITY
Faculty of Mechanical Engineering, Transport and Aeronautics
Institute of Transport

Pāvels Stankēvičs

Doctoral Student of the Study Programme “Transport”

**PRODUCTION TECHNOLOGY OF METAL
POWDER ANTIFRICTION PARTS FOR
ROLLING STOCK AND IMPROVEMENT OF
THEIR TRIBOLOGICAL PROPERTIES**

Summary of the Doctoral Thesis

Scientific supervisors:

Professor Dr. habil. sc. ing.
VIKTORS MIRONOVS

Asoc. Professor Dr.sc.ing.

DIJS SERGEJEVS

RTU Press
Riga 2020

Stankēvičs, P. Production Technology of Metal Powder Antifriction Parts for Rolling Stock and Improvement of their Tribological Properties. Summary of the Doctoral Thesis. Riga: RTU Press, 2020. 61 p.

Printed in accordance with the decision of the Promotion Council of Construction and Transport engineering "RTU P-22" of January 22, 2020, Minutes No. 01-1/2020.

<https://doi.org/10.7250/9789934225192>

ISBN 978-9934-22-518-5 (print)

ISBN 978-9934-22-519-2 (pdf)

DOCTORAL THESIS PROPOSED TO RIGA TECHNICAL UNIVERSITY FOR THE PROMOTION TO THE SCIENTIFIC DEGREE OF DOCTOR OF SCIENCE

To be granted the scientific degree of Doctor of Science (Ph. D.), the present Doctoral Thesis has been submitted for the defence at the open meeting of RTU Promotion Council on _____, 2020 at _____ at the Faculty of Mechanical Engineering, Transport and Aeronautics of Riga Technical University, _____ Street, Room _____.

OFFICIAL REVIEWERS

Researcher Ph. D. Dmitrijs Goljandins
Tallinn University of Technology, Estonia

Deputy Director for Science Ph. D. Vadims Savičs
Powder Metallurgy Institute, Belarus

Professor Dr. habil. sc. ing. Mārtiņš Kleinhofs
Riga Technical University, Latvia

DECLARATION OF ACADEMIC INTEGRITY

I hereby declare that the Doctoral Thesis submitted for the review to Riga Technical University for the promotion to the scientific degree of Doctor of Science (Ph. D.) is my own. I confirm that this Doctoral Thesis has not been submitted to any other university for the promotion to a scientific degree.

Pāvels Stankēvičs..... (signature)

Date:

The Doctoral Thesis has been written in Latvian. It consists of Introduction, 4 chapters, Conclusions, 69 figures, 16 tables, 8 appendices. The total number of pages is 151. The bibliography contains 101 titles.

CONTENTS

GENERAL CHARACTERISTICS OF THE DOCTORAL THESIS.....	6
Topicality of the Research.....	6
Research Problem.....	7
Aim and Tasks of the Doctoral Thesis	7
Research Methods	8
Research Equipment.....	8
Scientific Novelty of the Doctoral Thesis	9
Results of the Research Presented for the Defence	9
Practical Application of the Doctoral Thesis.....	9
LIST OF PUBLICATIONS	11
AUTHOR’S CONTRIBUTION TO PUBLICATIONS	13
APPROBATION OF THE DOCTORAL THESIS.....	15
LIST OF ABBREVIATIONS	16
1. PRODUCTION TECHNOLOGY OF METAL POWDER MATERIALS AND ITS APPLICATION IN RAILWAY TRANSPORT.....	17
1.1. Characteristics of Metal Powder Materials	17
1.2. Powder Types and Their Properties.....	18
1.3. Effects of Alloying Elements on the Properties of Parts	18
1.4. Assessment of the Use of Metal Powder Parts in Rolling Stock Components.....	20
1.5. Production of Metal Powder Parts.....	24
1.5.1. Analysis of Metal Powder Part Pressing	24
1.5.2. Sintering of a Metal Powder Blank Part.....	27
2. RESEARCH ON PRODUCTION PROCESSES OF EXPERIMENTAL METAL POWDER PARTS.....	30
2.1. Tribotechnical Characteristics of Experimental Low-Alloyed Parts.....	30
2.1.1. Mechanical Properties of Experimental Parts	30
2.1.2. Measurements of Tribological Properties and Surface Quality of Experimental Parts.....	33
2.3. Study of Densification in Pulsed Magnetic Field.....	36

3. METAL POWDER PARTS PRODUCTION DEFECTS AND QUALITY CONTROL MEASURES	39
3.1. Sintering Defects and Defect Reduction Measures	39
3.2. Ultrasound Quality Control of PM Parts	39
3.3. Control of PM Part Connections With the Help of Ultrasound and Radiography	41
4. RESEARCH ON SECONDARY OPERATIONS.....	46
4.1 Determination of Optimal Parameters for Mechanical Treatment of Porous Metal Powder Components	46
4.2. Enhancing the Antifriction Properties of Metal Powder Parts	51
4.2.1. Impregnating Porous Powder Parts	51
4.2.2. Disperse Medium and Disperse Components.....	51
4.2.3. Friction Coefficient Reduction Studies	53
CONCLUSIONS.....	55
BIBLIOGRAPHY OF THE SUMMARY.....	57

GENERAL CHARACTERISTICS OF THE DOCTORAL THESIS

Topicality of the Research

In the conditions of higher speeds of rolling stock and higher load capacity of cars, the work intensity of brakes is increasing as well, leading to higher wear at friction joints of the brake lever mechanism. As a consequence of wear, cracks can appear in pin joints of the brake lever mechanism, exceeding the allowed norms significantly and resulting in a lower pressing force of the brake pad and lower braking force of the train.

To improve operation of the brake lever mechanism of cars and to reduce their routine maintenance and repair costs, antifriction bushings are installed in pin joints of the brake lever mechanism.

Wear intensity of parts in the lever mechanism pin joints deteriorates their working conditions and causes the need for frequent adjustment and repair, which can lead to both premature wear of components of the structure itself and locking of the entire structure as a whole. As a result of earlier studies, it has been established that wear of parts of the brake lever mechanism is caused by vertical dynamic shock forces [46].

Since 2012, the PM sector has achieved significant progress in the treatment of composite alloys of ferrous metals, aluminium, titanium, magnesium and metals. The density of components continues increasing alongside with the improvement of powders, lubricating materials, equipment, warm sealing, large-capacity presses and sintering technology [25]. Powder metallurgy has developed rapidly in recent years due to the improved safety, strength, and hardness of manufactured parts, as well as the possibilities for producing large-size products and the widespread introduction of additive technologies in powder metallurgy. Due to its unique properties, the powder metallurgy technology is often used to manufacture antifriction products, such as sliding bearings, slide-blocks, bushings, etc. Nanotechnologies are being used and new solutions are being searched for to improve antifriction properties of metal powder parts [11]; thus, there are ongoing studies on increasing tribotechnical properties of metal powder antifriction parts.

The process of further usage of antifriction parts will be largely determined by their endurance and tribotechnical characteristics. Metal powder antifriction parts and their usage on the brake lever mechanism of rolling stock must comply with the enhanced requirements, such as wear resistance, durability, and safety, ensuring antifriction properties of the parts in a wide range of temperatures. Friction reduction in antifriction components is an urgent task [25].

The powder metallurgy (PM) process is a recognised method used today for large-scale production of various parts by economic means. Regular requirements for improving mechanical and tribological properties of parts to be manufactured are opposed to different trends in PM production, for example, in the form of a careful approach to the composition of alloying elements.

Traditionally, steel in PM is alloyed with Ni, Mo, and Cu; however, high prices, particularly for the first two, combined with risks to health related to Ni [1], lead to the fact

that PM industry is exploring the possibilities for reducing the share of these alloying elements [5], as well as the possibility of using other alloying elements. Therefore, new solutions are needed to create safe, economically viable metal powder materials with appropriate tribotechnical characteristics.

Research Problem

In the Doctoral Thesis, metal powder antifriction parts with low alloying element content are studied in order to assess their suitability for use in the brake lever mechanism of cars. Since the alloying element content largely determines the price of metal powder, the competitiveness of these parts will be achieved. On the other hand, by reducing the content of the alloying elements in the powder mixture, the strength and endurance parameters of parts may also be reduced; thus, studies are needed on the suitability of these parts for their use in the brake lever mechanism of the rolling stock.

When using powder parts in the most significant components, it is necessary to verify the quality of parts. The types of a non-destructive control test are mainly oriented and approved on parts obtained by other production methods (casting, forging) [31]; thus, studies have been performed in the Thesis to check their suitability for porous metal powder parts. In spite of the fact that powder metallurgy positions itself as a production which does not require additional operations after part manufacturing, still secondary operations, such as mechanical treatment, are required in some cases [4]. It is important to foresee the changes in the surface roughness of parts when using mechanical treatment for metal powder parts.

The issue of increasing antifriction properties is topical, as, with reduction of the friction factor, more favourable working conditions for antifriction parts will be achieved that will in turn ensure safer operation of parts with low-alloyed elements in antifriction components.

Aim and Tasks of the Doctoral Thesis

The Aim of the Doctoral Thesis is research of the production technology of metal powder antifriction materials and promotion of tribotechnical properties of low-alloyed antifriction parts for use in rolling stock components.

The following tasks have been set to achieve the aim:

- 1) to research the technological process of production of metal powder parts;
- 2) to analyse properties of metal powder materials and their benefits for use in railway transport;
- 3) to evaluate the suitability of metal powder antifriction parts based on Fe-C-Cu with low alloying element content to be used in the brake lever mechanism of rolling stock;
- 4) to perform pressurising studies of metal powder material with pulsed magnetic field;
- 5) to evaluate the appropriateness of non-destructive control for monitoring the quality of antifriction parts;
- 6) to determine optimal parameters for mechanical processing of porous metal powder sliding bushing;

- 7) to develop a method for reducing the friction factor for antifriction metal powder parts with the use of WS₂ and WSe₂ nanoparticles.

Research Methods

- Analysis of literature, scientific articles and other information presented in various international publications and scientific journals.
- Systemic analytical methods to study causal relationships between various components of powder compositions and to reveal the factors contributing to the tribotechnical properties of the material.
- Empirical experimental studies with metal powder materials and antifriction parts.
- Comparative method for analysing the characteristics of the parts to be studied at different stages and conditions of the research.
- Methods of mathematical numerical analysis. Method of final elements for mechanical processing of low-alloyed metal powder bushings.
- Statistical methods of data processing for analysis of the results obtained. Analysis of theoretical and experimental studies, drawing up conclusions and recommendations.

Research Equipment

The following equipment has been used to assess the properties of metal powder antifriction materials.

- For tribotechnical studies – *Taylor Hobson Ltd.* 3D measurement system and *CSM Instrument Ball-on-disk tribometer*.
- For metallography – PRESI equipment: *Mecatome 255/300*, *Mecapress II*, *Mecatech 334* and microscope *Keyence VHX-2000*.
- For combined (magnet-pulse) technology studies – experimental magnet-pulse pressing equipment of RTU Powder Material Scientific Laboratory and *Impulse magnetizer U-series*.
- For non-destructive tests – *USM 25 of Krautkramer GE Inspection Technologies GmbH* and *X-ray SMART EVO 200D of YXLON*.
- For mechanical treatment studies – *Okuma L200 E-M*.
- Experimental laboratory equipment for testing friction and wear of materials.
- The results of experimental studies have been graphically displayed by using Microsoft Excel, Microsoft Word and SolidWorks software.
- Statistical relevance of the results and factors obtained from the research has been assessed by using *Excel Data Analysis* and *Minitab* application programs.

Scientific Novelty of the Doctoral Thesis

1. It has been demonstrated that when manufacturing antifriction metal powder parts, the reduction of the content of the Ni and Mo alloying elements can be compensated by improving their tribological properties by impregnating them with WS₂ and WSe₂ nanoparticles.
2. Effects of cutting modes of porous powder parts on the roughness properties of the treated surface have been determined.
3. For the first time, the method of reducing the friction coefficient has been experimentally proven for low-alloyed metal powder sliding bushings used in the car brake levers by impregnating them with WS₂ and WSe₂ nanoparticles (LV Patent No. 15433).

Results of the Research Presented for the Defence

1. Porous antifriction metal powder material with a low content of alloying elements was developed to manufacture antifriction sliding bushings of the brake lever mechanism of a car.
2. Mechanical treatment methodology for porous antifriction metal powder material was developed.
3. Method of improving the tribological properties of metal powder antifriction material by using WS₂ and WSe₂ nanoparticles was developed.

Practical Application of the Doctoral Thesis

Test samples of antifriction metal powder bushings with the reduced content of alloying elements have been manufactured and studied. Powder mixtures with reduced content of alloying elements allow reducing costs for the manufacture of antifriction bushings. It has been demonstrated that tribotechnical characteristics of test samples meet the requirements for the use in the brake lever mechanism of a car.

Following the results of the research of porous metal powder parts with the use of non-destructive testing it has been proven experimentally that ultrasound and radiographic microscopy methods allow for a qualitative detection of defects in sintered powder parts, as well as the continuity of connection of metal powder inserts after their compression with pulsed magnetic field.

Practical knowledge has been obtained, certain characteristics and prospects for pressing powder parts with pulsed magnetic field have been determined.

Methodology for mechanical treatment of porous powder parts has been developed. Experimental studies have allowed determining the optimal treatment cutting modes and establishing that roughness of the treated surface depends on the cutting rate rather than on the feed rate.

Research has been performed to improve the tribotechnical properties and reduce the friction factor of antifriction powder parts; also, a method has been offered for impregnation

of metal powder bushings used in the braking system with oil containing tungsten disulphide and tungsten diselenide nanoparticles (WS_2 and WSe_2).

Experimental equipment for friction and wear testing in a wide range of temperatures has been designed and manufactured, and a technique and equipment for impregnating porous products with nanoparticles for which LV patents have been obtained.

The results obtained in the Doctoral Thesis open new opportunities for extensive application of metal powder technology, improvement of properties of antifriction materials, and quality control.

LIST OF PUBLICATIONS

The Doctoral Thesis is based on the scientific articles mentioned below and the research performed during writing of these articles, which are published in scientific periodicals and are internationally available in the scientific information data storage resources and quoted in internationally accessible databases.

1. Mironovs, V., **Stankevich, P.**, Eiduks, J. *Tendencies in the field of application of metal-powder materials for repair and maintenance of railway equipment*. ICTE in Transportation and Logistics 2019. Procedia Computer Science, 2019, vol. 149, pp. 344–348. ISSN 1877-0509. Available from: doi:10.1016/j.procs.2019.01.146
2. Mironov, V., **Stankevich, P.**, Tatarinov, A., Zemchenkov, V., Boiko, I. *Mechanical and Acoustical Properties of Bushings Made of Low-Alloyed Materials and Used in Brake Systems of Transport Vehicles*. Materials Science and Engineering, 2015, vol. 96, Iss. 1, pp. 1–9. ISSN 1757-8981. e-ISSN 1757-899X. Available from: doi:10.1088/1757-899X/96/1/012016
3. Tatarinov, A., Mironov, V., Rybak, D., **Stankevich, P.** *Non-Destructive Testing of Joints of Antifriction Parts Crimped by Pulsed Magnetic Deformation*. Solid State Phenomena, 2017, vol. 267, pp. 248–252. ISSN 1662-9779. Available from: doi:10.4028/www.scientific.net/SSP.267.248
4. Mironov, V., **Stankevich, P.**, Beljaeva, I., Glushenkov, V. *Static-Dynamic Powder Material Compaction Methods*. In: 15th International Scientific Conference “Engineering for Rural Development”: Proceedings. vol. 15, Latvia, Jelgava, 25–27 May 2016. Jelgava: Latvia University of Agriculture, 2016, pp. 1128–1132. ISSN 1691-5976
5. Mironovs, V., **Stankevics, P.**, Kromanis, A., Lungevics, J. *Influence of Machining Parameters on 3D Surface Roughness of Powder Bushings*. Key Engineering Materials, 2017, vol. 721, pp. 378–382. ISSN 1013-9826. e-ISSN 1662-9795. Available from: doi:10.4028/www.scientific.net/KEM.721.378
6. **Stankevich P.**, Mironovs, V., Vasilyeva, E., Breki, A., Tolochko, O. *The Possibility of Modifying the Elements of the Bearing Assembly with Nanoparticles in Order to Reduce the Friction Coefficient*. IOP Conference Series: Materials Science and Engineering, 2017, vol. 251, pp. 1–5. ISSN 1757-8981. e-ISSN 1757-899X. Available from: doi:10.1088/1757-899X/251/1/012084

Inventions

LV Patents

1. Riga Technical University. *Iekārta materiālu triboloģisko īpašību novērtēšanai.* (Equipment for testing the tribological properties of the materials). Viktors Mironovs, **Pāvels Stankēvičs**, Jānis Rudzītis, Int. Cl.:G01N3/56. Submission date: 29.12.2016. Patents and Trade Marks. LV15225. 20.12.2017.
2. Riga Technical University. *Paņēmiens un iekārta poraino izstrādājumu piesūcināšanai ar nanodaļiņām.* (The method and equipment for impregnation of porous parts with nanoparticles). Viktors Mironovs, Aleksandrs Polakovs, **Pāvels Stankēvičs**, Aleksandrs Korjajkins. Submission date: 28.12.2018. Patents and Trade Marks. LV15433. 20.02.2020.

AUTHOR'S CONTRIBUTION TO PUBLICATIONS

All attached scientific articles have been written by the author in cooperation collaboration with his scientific supervisor Professor V. Mironovs and other co-authors presented in of the articles. The work on performed in each article is was jointly planned by the all authors.

The author's contribution to the research presented in the attached articles consists of is as follows:

- all graphic presentations, analyses and preparations of all samples used for testing and measurement;
- characteristics of the researched materials, all metallography studies with respective previous preparation;
- performance of all analyses of the researched materials with the subsequent data assessment.

The following is the summary of the Author contribution to each article is as follows:

Publication I

The article highlights the main trends in the use of modern metal ceramic materials. The author has written and drafted the main part of the article and has performed an analysis of the use of metal powder materials in rolling stock components. Benefits of powder parts are shown and recommendations for reducing the friction factor of antifriction parts are provided.

Publication II

The author has studied the main characteristics and requirements for the production of antifriction bushings by using the powder metallurgy method. Effects of alloying elements on tribotechnical characteristics of the parts have been determined; the author has participated in implementing the test model for powder parts with the TOF method of a non-destructive test and in experimental research of the surface quality of parts. The author has substantiated the benefits of using low-alloyed powder compositions in brake lever mechanisms.

Publication III

In this article, measurements and testing with the help of UT, RT methods of a non-destructive test have been performed together with the co-authors. The author has performed the numerically analytical work, has determined the quality of the bushing connection after compression with a pulse magnetic field and has compared test methods, has and drawn up and drafted the article.

Publication IV

The author has designed experimental equipment using the resources of the RTU Powder Materials Laboratory to perform an experiment in pressing powder materials with a pulse magnetic field. Key pressing modes have been identified, the required measurements have

been made, and the author has participated in conducting the experiment and, has drawn up and drafted the article.

Publication V

Research on mechanical treatment of powder parts has been conducted jointly with co-authors. The author has determined the ranges of the mechanical treatment and has conducted a part of the experiments. The required theoretical and practical studies have been performed, as well as some measurements to determine roughness of the surface of the treated powder part. The author has analysed the morphology of turnings and has substantiated the cutting modes. The author has drawn up and drafted the article.

Publication VI

The author has developed a theoretical model and has conducted research on impregnation of samples of antifriction bushings with oil emulsions containing WS_2 and WSe_2 nanoparticles. Tribological measurements have been carried out; conclusions and recommendations have been made jointly with the co-authors. The author has written the main part of the article.

APPROBATION OF THE DOCTORAL THESIS

All results of this research have been presented and published at the seminars for doctoral students and international scientific conferences.

Article I

“Tendencies in the field of application of metal-powder materials for repair and maintenance of railway equipment” – results of the research were published in the scientific journal “ICTE in Transportation and Logistics 2018” in 2018 (ICTE 2018).

Article II

“Mechanical and Acoustical Properties of Bushings Made of Low-Alloyed Materials and Used in Brake Systems of Transport Vehicles” – results of the research were presented at the 2nd International Conference on Innovative Materials, Structures and Technologies, in Riga, Latvia, 30 September – 2 October 2015, and published in IOP Conf. Series: Materials Science and Engineering (vol. 96).

Article III

“Non-Destructive Testing of Joints of Antifriction Parts Crimped by Pulsed Magnetic Deformation” – results of the research were presented at the 26th International Baltic Conference of Materials Engineering, in Kaunas, Lithuania, 26–27 October 2017, and published in scientific journal Solid State Phenomena (vol. 267).

Article IV

“Static-Dynamic Powder Material Compaction Methods” – results of the research were presented at the 15th International Scientific Conference Engineering for Rural Development, in Jelgava, Latvia, on 25–27 May 2016, and published in scientific journal Agronomy Research (vol.14).

Article V

“Influence of Machining Parameters on 3D Surface Roughness of Powder Bushings” – results of the research were published in scientific journal Key Engineering Materials, December 2016 (vol. 721).

Article VI

“The Possibility of Modifying the Elements of the Bearing Assembly with Nanoparticles in Order to Reduce the Friction Coefficient” – results of the research were presented at the 3rd International Conference on Innovative Materials, Structures and Technologies, in Riga, Latvia, 27–29 September 2017, and published in IOP Conf. Series: Materials Science and Engineering (vol. 251).

LIST OF ABBREVIATIONS

ANOVA – analysis of dispersion (Analysis of Variance)

BC – brake cylinder

BLM – brake lever mechanism

FEM – finite element method

MIP – magnetic impulse pressing

MT – magnetic ferro-particle test

PM – powder metallurgy

PT – penetration test

SPM – sintered powder materials

TEM – transmission electron microscope

tf – tonne of force

TOF – time of flight method

UT – ultrasound test

VT – visual test

1. PRODUCTION TECHNOLOGY OF METAL POWDER MATERIALS AND ITS APPLICATION IN RAILWAY TRANSPORT

1.1. Characteristics of Metal Powder Materials

Powder metallurgy technology includes the manufacture of powders, moulding, sintering and mechanical treatment of powder parts as needed after finishing operations. Basic parameters of manufacturing parts are the force of pressing and ways of implementing it, the temperature mode of sintering, the environment and the speed of the process. The production technology of metal powder products is constantly developing and improving.

There are porous materials containing 10–30 % residual porosity after final treatment and compact powder materials where porosity amounts to a maximum of 3–5 % [14], [23].

Antifriction materials are a group of materials with a low friction factor or materials capable of reducing the friction factor of other materials. Solid anti-friction materials have increased resistance to wear in the event of prolonged friction [19].

There are different types of metal powder sliding bearings and sliding bushings manufactured (Fig. 1.1), which are notionally subdivided into two groups:

- oil-impregnated bearing containing lubricant due to porosity properties of metal powder parts;
- dry bearing consisting of solid lubricant (graphite), which reduces friction without oil supply.



Fig. 1.1. Powder material sliding bushings [54].

Oil-impregnated bearings made from powder alloys may operate without forced lubrication due to the “perspiration” of oil from the pores [8], [50].

Friction materials have a high friction factor during contact with metallic surface; they are used in brakes and shaft friction clutches.

1.2. Powder Types and Their Properties

Powders to be used in the manufacture of parts should meet the specific characteristics and requirements that affect their technological appropriateness. These characteristics and requirements are:

- high density of the embankment (to ensure increased mass and density of the body);
- good flowability (to ensure rapid filling of the extrusion form);
- high plasticity (to ensure maximum density) [15].

The industry produces a variety of metal powders: iron, copper, nickel, chromium, cobalt, tungsten, molybdenum, titanium, etc. Methods of obtaining powders are conditionally classified into mechanical and physical-chemical [9].

1.3. Effects of Alloying Elements on the Properties of Parts

The use of pure iron powder as a raw material in the manufacture of powder parts is limited because tenacity properties of sintered iron are low [9]. Nickel, copper, chromium, molybdenum, etc., are used as alloying elements. The role of each is determined by the quantitative ratio of the alloying element to iron and other alloying elements, as well as by the ratio of oxides representing in most cases the boundaries between particles.

Regarding the ratio to carbon in steel, alloying elements are divided into:

- carbide forming,
- graphite forming.

The impact of alloying elements on pore healing kinetics and other defects in the crystal structure, as well as on the contracting of powder steel, is of importance.

In order to increase the contraction and mechanical properties of powder products, it is appropriate to introduce elements into the powder mixture that form low-melting eutectics during sintering with iron, liquid solutions, etc., activating the sintering process. Best results are achieved by alloying complexes with carbon, copper, nickel, molybdenum, and other elements [36].

It has been established [48] that nickel, as well as a number of other elements, and in particular copper (in liquid state), contribute to the “absorption” of the borders between particles, the formation of a metal contact between particles, redirection of collecting cross-particle recrystallisation, which, on the one hand, increase mechanical properties of the sintered products and, on the other hand, decrease the resilience of austenite to the growth of its grains during both the process of sintering and heating during the isothermal treatment. On the contrary, elements such as chromium, silicon and manganese, which make it difficult to reduce oxides on the surface of particles, prevent fusion of particles and, in order to perform cross-particle re-crystallisation, sintering products, well dried and purified from oxygen and moisture, are required. Therefore, simultaneous alloying of powder materials with carbide-forming and non-carbide-forming elements is appropriate by adding them to a powder mixture such as the ligature powders of CuSi, CuMn, and MnNi type.

On the one hand, addition of graphite significantly reduces the mechanical strength of the material, and on the other, the presence of graphite in the furnace charge allows for a smoother density of the products due to better powder fluidity and tightness (Fig. 1.2). Graphite eliminates dry friction and promotes absorption of vibration [43].

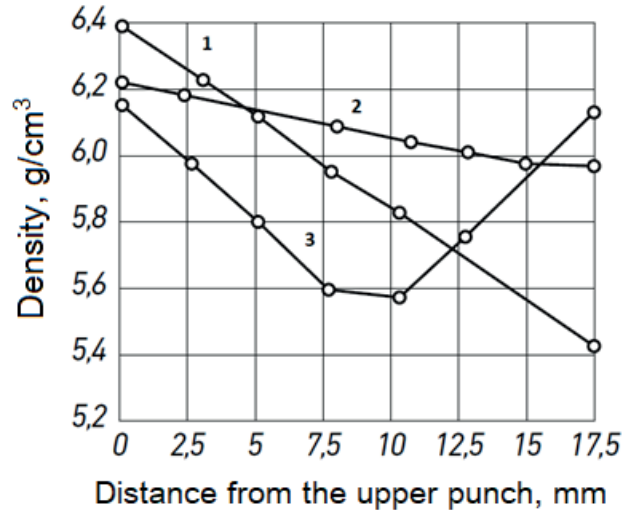


Fig. 1.2. Density in extrusion areas at the distance from the upper punch.

- 1 – copper for one-sided extrusion;
- 2 – copper with 4 % graphite for one-sided extrusion;
- 3 – copper for double-sided extrusion without added graphite.

Graphite crystal lattice is formed by parallel two-dimensional layers located at a distance of 0.34 nm from each other. Each of these layers consists of carbon atoms placed on the peaks of correct hexagonals (hexagon crystal lattice) [37].

Mechanical properties of a metal powder material depend to a large extent on the microstructure of the material, which in turn depends on the chemical composition of the powder mixture, particularly the contents of the alloying elements [24]. Figure 1.3 shows the extent to which the contents of the alloying elements affect iron hardness.

Powder iron alloying with only nickel is rare; moreover, a significant improvement of properties is observed only at high sintering temperatures, which in turn leads to increased consumption of energy resources during the sintering process. Increasing of the nickel content in steel lowers the optimal carbon content and decreases hardness of steel (Fig. 1.3). In order to obtain products with high mechanical properties, alongside with nickel, powder steel is alloyed with copper and other alloying elements.

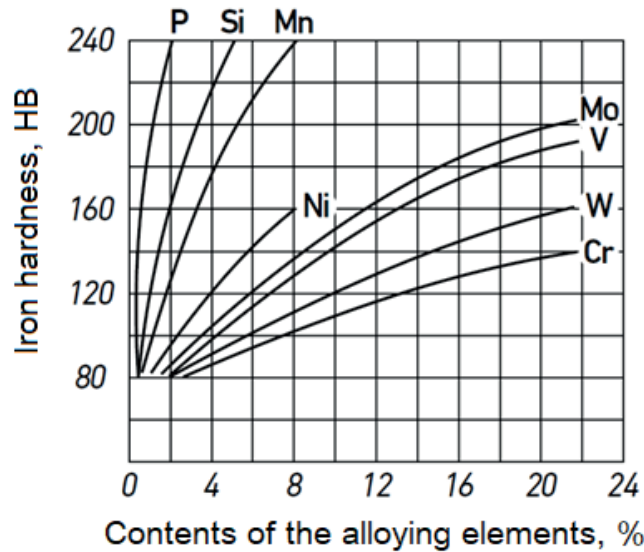


Fig. 1.3. Effects of alloying elements on iron hardness (HB).

1.4. Assessment of the Use of Metal Powder Parts in Rolling Stock Components

Metal powder parts used in rail transport typically have a significantly higher mass and size compared to the parts used in other sectors. They can be divided into different groups: structural, antifriction, friction and electrical. Structural parts can be water and oil pump driving gears and sliding bushings (Fig. 1.4) [19].



Fig. 1.4. Sliding bushings of the brake lever mechanism [19].

Regarding antifriction parts, sliding bushings are most extensively used in rail transport. They have a number of advantages: economic operation, since the use of this type sliding bushings allows reducing oil consumption, decreasing production costs and saving material, since it is possible to use iron-copper powder material instead of expensive bronze and Babbitt, as well as high wear resistance provided by the self-lubrication effect.

The wider group is composed of car and locomotive friction parts (Fig. 1.5). They are made in the form of discs, sectors and blocks on an iron and copper basis and are intended to

be used in brake mechanisms, friction clutches and other equipment operating in dry and liquid friction conditions.

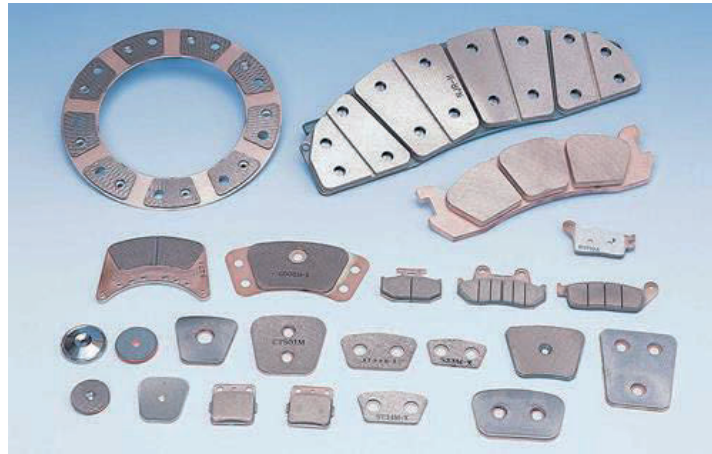


Fig. 1.5. Friction parts on an iron and copper basis [19].

The most common PM parts used in railway rolling stock are brake pads and anti-friction sliding bushings. Metal powder bushings are used in pin joints of brake lever mechanisms of cars. Freight cars are equipped with braking systems, placed on the truck and frame of a car. Such layout has both advantages and disadvantages.

Advantages: all elements of pneumatic parts of the brake are connected to each other with secure metal pipes and attached to the frame of a car.

Disadvantages: a large volume of mechanical parts, a large number of moving elements each of which may need to be replaced or repaired, the overall reduced efficiency of transmission by increasing depreciation of antifriction components.

Construction of the brake lever mechanism of a car

Safety of operation of the braking system is ensured by pneumatic and mechanical brake parts. The pneumatic part of the car brakes ensures the timely formation of force in the brake cylinder rod during the braking process. The mechanical part of the brakes ensures that the brake pads are pressed to and released from the rolling surface of wheelsets. In many cases, it is not possible for design reasons to ensure that the brake cylinder rod is pressed directly to the friction elements. Consequently, the need to introduce a brake lever mechanism is dictated by the functional and constructive features of the braking system.

The brake lever mechanism (BLM) of a gondola car, model *12-132-03* – the specific model used by Latvian railways – has been considered as a construction under research, where antifriction metal powder bushings are used [55].

BLM serves for force supply from the brake cylinder (BC) rod to brake pads with a certain increase of force and its even distribution to wheelsets (Fig. 1.6).

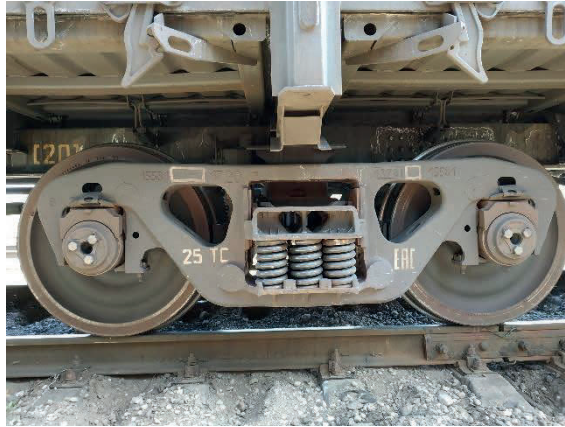


Fig. 1.6. Single-action BLM – car truck view.

The BLM is characterised by the ratio of the total pressure force and air pressure of all brake pads in BC. The ratio describes the number of times the brake pad pressure force exceeds the BC air pressure force [40].

For the purpose of simplifying repair and extending service life, the brake lever joint connections are fitted with wear-resistant bushings made by using the powder metallurgy method [47].

The use of antifriction material in the roller – bushing component – allows [53]:

- to increase the service life of joint components of the brake lever mechanism;
- to decrease wear of the counter-body (roller);
- to maintain a constant compressive force of the brake pads during their operation;
- to save materials used for service and maintenance.

The four-axle brake lever mechanism of a freight car is shown in Figure 1.7 [55].

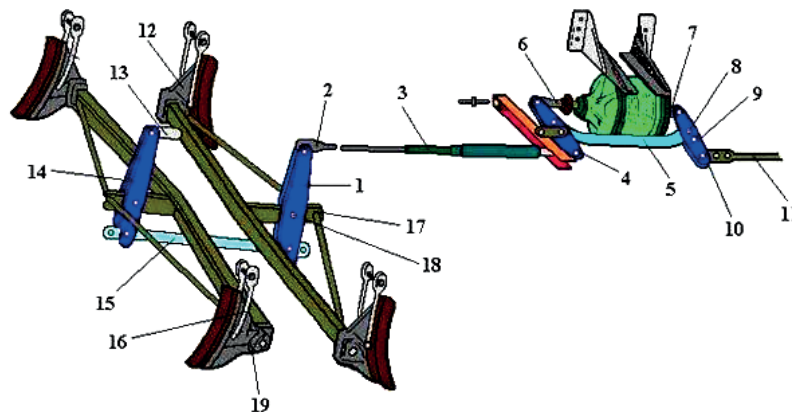


Fig. 1.7. Brake lever mechanism of a freight car [55].

Operation principle of a brake lever mechanism

Brake cylinder piston rod 6 and stress point bracket 7 are coupled by rollers with horizontal levers 10 and 4, which are connected to each other in the middle part by coupling rod 5. Coupling rod 5 is installed in aperture 8 in the case of composition brake pads or in aperture 9 in the case of cast iron brake pads. Levers 4 and 10 are coupled from opposite ends

with rollers through traction unit 11 and automatic regulator 3. Lower ends of vertical levers 1 and 14 are linked to each other with spreader 15, while the upper ends of lever 1 are connected to traction unit 2, upper ends of outside vertical levers 14 are attached to the truck frames by means of tow bar 13 and brackets. Triangular spindles 17, on which shoes 12 with brake pads are fitted, are connected by rollers 18 to vertical levers 1 and 14. Safety corners 19 and braces are designed to avoid drop of triangular spindles and spreaders on the road in the event of their detachment or rupture. Brake shoes and triangular spindles 17 are attached to truck frame on suspensions 16. Controller tow bar 3 is connected to the lower end of the left horizontal lever 4 and regulating screw is connected to traction unit 2. During braking, the body of regulator 3 leans against the lever connected to the horizontal lever 4 with a coupling rod. Antifriction metal ceramic bushings use pin joints of the vertical lever, as provided in Figure 1.7, denominated as 1 and 14. The bushings are installed in the vertical levers and their coupling rod (Fig. 1.8).

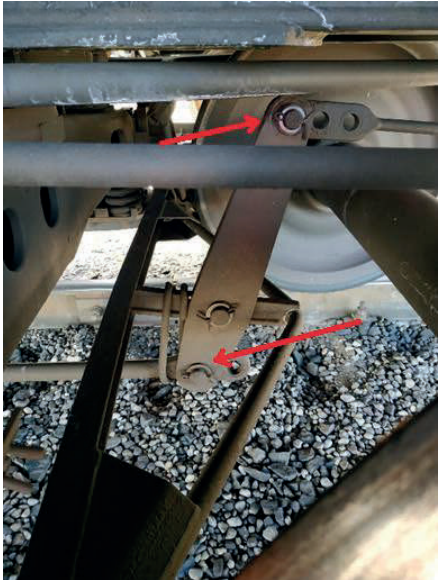


Fig. 1.8. Vertical lever of the brake lever mechanism of a freight car (arrows denote mounting points).

Exploring modern trends in the use of metal powder materials in rolling stock parts, the author has come to the conclusion that the variety of properties and capabilities of metal powder materials allow them to be used in different components of rolling stock. In rail transport, powder metallurgy is most widely used in the manufacture of antifriction sliding bearings, bushings, slide-block and contact plates, as well as friction blocks.

Latvian Railways most often use metal powder antifriction bushings that are installed in the vertical levers of the brake lever mechanism of a freight car.

1.5. Production of Metal Powder Parts

1.5.1. Analysis of Metal Powder Part Pressing

The goal of compacting is to fabricate a blank part of a certain shape, size and strength out of a powder batch. During compaction the contact between powder particles increases, the porosity decreases, separate particles become deformed or damaged.

The strength of a produced blank part is a result of mechanical coupling (cohesion) and of the action of electrostatic friction and gravity forces. As the compaction pressure increases, the relative density increases too, which results in the growth of a blank part hardness and durability Figure 1.9.

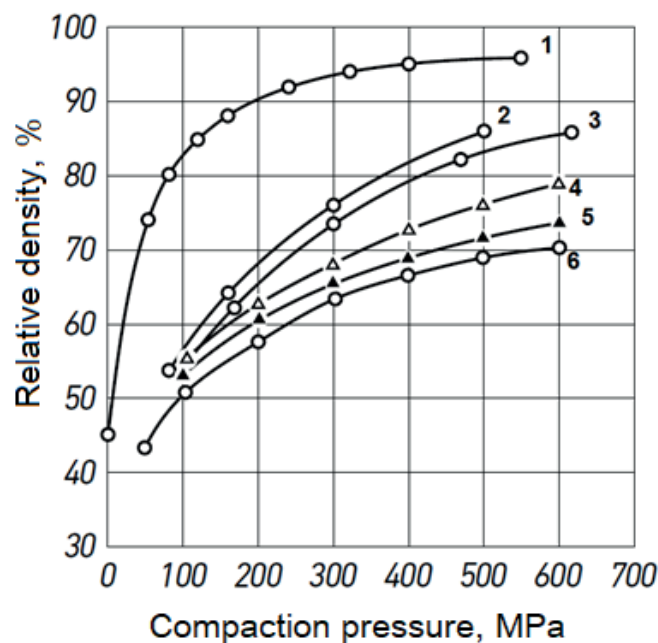


Fig. 1.9. Correlation between the metal powder compaction pressure and relative density:
1 – Al; 2 – electrolytic Cu; 3 – porous Fe; 4 – electrolytic Fe; 5 – Fe carbonyls;
6 – H₂- reduced W [29].

As the density increases (along with the decrease of porosity) by 1 %, the compaction pressure normally grows by 3–4 %. Unilateral compaction is the most widespread PM compaction technique. The powder being mixed with lubricants and graphite, fills a matrix cavity and is compacted by moving the punch axis, the compaction pressure normally is in the range from 400 MPa to 1200 MPa. Sometimes high compaction pressure also causes cold densification of particles, which provides sufficient durability for further treatment [64].

Changes in the volume of a powder compact during compaction occur due to the process of compression. Density of a blank part depends on the compaction pressure. Conversion processes during powder compaction are shown in Figure 1.10 [24], [57].

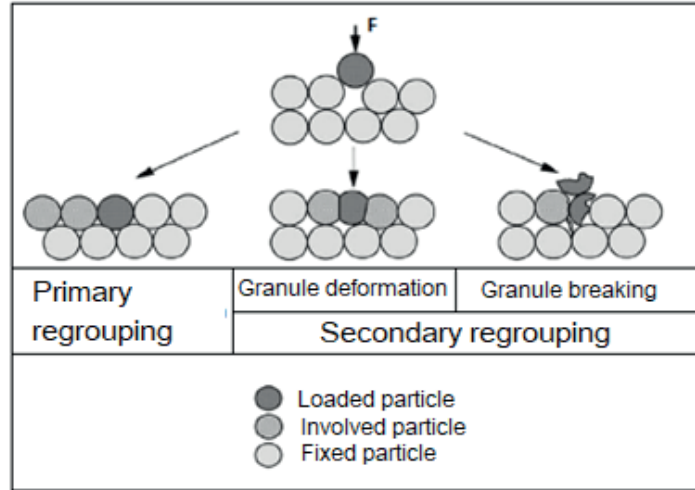


Fig. 1.10. Particle conversion processes during compaction.

Hard granules are difficult to deform, and this can lead to a lower density at the given densification pressure. Still, if granules are too soft, they will slightly deform in response to the applied pressure, but will not convert to the required degree at a low pressure. Some compaction cavities, which have not been fully filled in at the stage of deformation, remain, and big density gradients will appear under unilateral compaction [10]. Ideally, granules should be regrouped and deformed during densification. [26].

While being compacted, the powder compact is compressed in all directions. Lateral pressure makes 25–40 % of the compaction pressure, and it can be calculated using Equation (1.1) [44]:

$$P^r = \xi p, \quad (1.1)$$

where P^r is specific lateral pressure, kg/cm^2 ; p is specific compaction pressure, kg/cm^2 ; and ξ is lateral pressure coefficient.

The lateral pressure coefficient depends on physical powder characteristics: plasticity, dispersive capacity and particle shape. Lateral pressure is measured by the height of a compacted blank part, and it decreases due to axial pressure fall.

Total pressure on a powder blank part P , positioned in a cylindric dye with relative density θ , known height h and relative compaction pressure p can be calculated using Equation (1.2):

$$P = \frac{\pi D^2}{4} p, \quad (1.2)$$

as soon as lateral surface pressure per 1 cm^2 is $P^r = \xi p$, and lateral surface area is πDh , total pressure on it will amount to:

$$P^r = \xi \pi Dh p = \xi \pi D h_r p, \quad (1.3)$$

where h_r is reduced height of the blank part, mm.

So, total lateral pressure depends only on the value of the specific vertical pressure, but all other values are constant for the current powder dose by weight.

Under unilateral compaction (Fig. 1.11), the density of the blank part ρ decreases in the compaction direction.

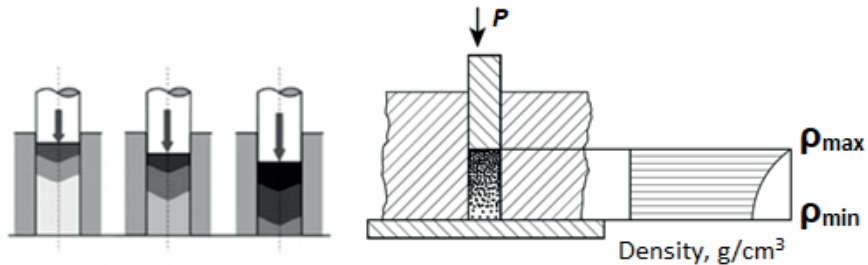


Fig. 1.11. Position of the density of the blank part along the height under unilateral compaction.

Bilateral compaction (Fig. 1.12) is used if sizes of a fabricated part correspond to the requirements of formula (1.4) or (1.5).

$$1 < \frac{h}{d} < 5, \quad (1.4)$$

$$3 < \frac{h}{s} < 17, \quad (1.5)$$

where h is workpiece height, d is diameter, and s is wall thickness.

Under bilateral compaction, which provides more even distribution of the material density, two punches moving towards each other during compaction are used, and the material density fall is observed in the middle of the blank part (Fig. 1.12).

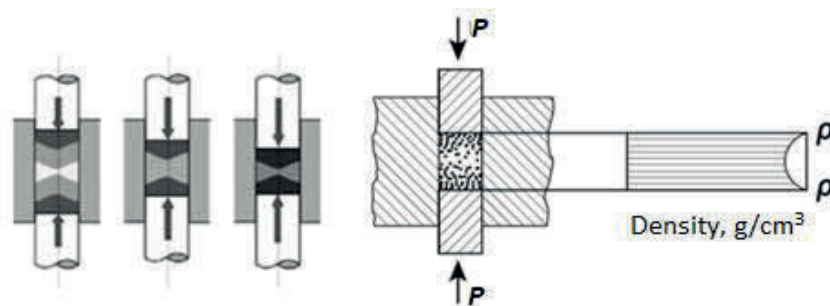


Fig. 1.12. Position of a blank part density after bilateral compaction.

Dies are used to form internal openings, similar to design of the ones in Figures 1.11 and 1.12, enhanced with pin bars.

Table 1.1 shows pressure values under unilateral compaction and the main modes of technological operations aimed at achieving the required density of a workpiece.

Table 1.1

Main Modes of Technological Operations for Fabrication of Work Pieces With
the Required Density [3], [52]

Density, g/cm ³	Modes of technological operations
6.0–6.6	Compaction pressure 500–700 MPa, sintering temperature 1150–1200 °C, time – 2 hours
6.7–7.1	Compaction pressure 400–600 MPa; I sintering: temperature 800–850 °C, time – 1 hour; extra compaction at pressure 600–000 MPa; II sintering: temperature 1150–1200 °C, time – 2 hours
7.2–7.5	Compaction pressure 400–600 MPa, sintering at temperature 1150–1200 °C, time – 2 hours, heating up to 1100 °C and stamping at pressure 800–1000 MPa
7.6–7.8	Compaction pressure 600–700 MPa, sintering at the temperature 1100–1200° C, time – 2 hours including impregnation with copper or brass

1.5.2. Sintering of a Metal Powder Blank Part

Cold pressing does not provide sufficient mechanical hardness of a blank part. To enhance physical and technical characteristics and to provide for the physical and chemical properties of parts, the blank parts are subjected to sintering. Sintering occurs at the temperature 0.7–0.8 of the absolute basic component melting temperature [3]. During sintering, density and hardness of workpieces increase, the required physical and chemical properties are achieved [22].

Sintered powder compacts are characterised by some geometrical elements (Fig. 1.13), which could be defined with such notions as “neck”, “interparticle contact”, “pore”, etc.

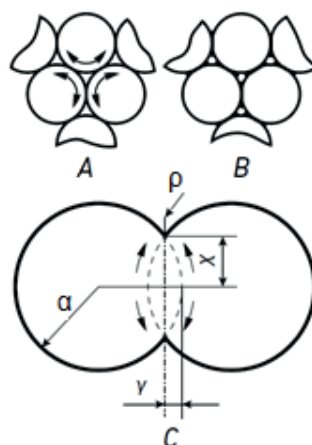


Fig. 1.13. Fragment of a powder compact before (A) and after (B) sintering and a two-dimensional sintering model (C): α – particle radius; ρ – “neck” radius; χ – cross-sectional radius of the circle of contact of the particles; γ – half of the distance between the particle centres (proximity).

J. Geguzins [41] distinguished three fundamentally different states of a powder compact during its heating, each of them corresponding to a certain stage.

- During the *first* (initial) stage, sintering of the powder particles to each other occurs along with the contact area growth between them; each particle retains structural individuality, i.e., the boundary between them remains and, consequently, the notion “contact between the particle” remains too.
- During the *second* stage, the porous compact can be described as two randomly variable phase arrays – substance (particles) phase and “void” (pores) phase, at this stage closed pore formation is not finished yet, but contacts between particles are already lost and boundaries between them appear to be positioned arbitrarily, with no connection to the initial boundary positioning between initial particles.
- During the *third* stage, in the powder compacts there are only mainly closed, isolated pores, the number and total volume of which may decrease. It should be noted that even these three highly generalized stages cannot be clearly delineated: closed (isolated) pores collide in a real powder compact at an early heating stage (for instance, already during fabrication of a blank part), but some initial contacts between the particles remain almost until the third sintering stage.

Powder conglomerate conversion process in a dense compact can be considered as the analogue for a chemical reaction and characterised using the thermodynamic equation of free energy decrease (1.6) [67]:

$$\Delta F = \Delta H - T\Delta S, \quad (1.6)$$

where ΔH and ΔS are corresponding changes in the thermal capacity and system entropy.

Indicative modes of powder antifriction material compaction and sintering are specified in Table 1.2.

Table 1.2

Powder Antifriction Material Compaction and Sintering Modes [9]

Powder material	Compaction pressure, MPa	Sintering mode		
		Temperature, °C	Holding time, min	Protective medium
Ferrum graphite	400–800	1050–1150	60–180	Endogas
Bronze graphite	200–400	720–850	30–120	Hydrogen

At the initial stages of sintering, the interconnected surface-open pores are also necessary. Open pores are necessary to efficiently remove the lubricants and to provide the output of gaseous products (for example, water steams) under early iron oxide recovery, which is important for interparticle neck formation (Fig. 1.14).

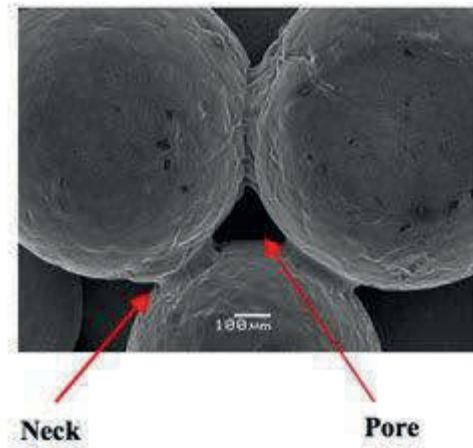


Fig. 1.14. Formation of the necks and pores [56].

Formation of the neck starts from interparticle contact and increases along with the rising of temperature, thus creating a continuous network. Due to diffusion, resistant interparticle necks are formed, which are necessary to provide good mechanical properties of the material.

2. RESEARCH ON PRODUCTION PROCESSES OF EXPERIMENTAL METAL POWDER PARTS

2.1. Tribotechnical Characteristics of Experimental Low-Alloyed Parts

2.1.1. Mechanical Properties of Experimental Parts

For the purposes of detailed research of tribotechnical properties of antifriction parts, the experimental samples of bearings in brake lever system were fabricated from low-alloyed Fe-C powder mixes. The parts were fabricated using unilateral static compaction, followed by sintering.

Samples were fabricated from powder mixes containing such alloy components as Ni, Cu, Mo (Table 2.1). Hognas AB mix AHC100.29 + Cu + Ni + C (mix 1) was certified as the basic propagating material along the mix with Ni and Mo content lower than 0.3 % and increased Cu content (Mix 2) and Mix 3 with Ni content above 2 % [57].

Table 2.1

Characteristics of Materials for Sample Fabrication

Mixture	Components, [Mass concentration, %]								Powder characteristics		
									Flowability, s per 50 g	Bulk density, g/cm ³	Densification, g/cm ³
	Fe, %	Ni, %	Cu, %	Mo, %	S, %	P, %	C, %	Ken- nolube			
Mix 1	94	2.0	2.0	0.5	0.2	0.1	1.2	1.0	38	3.18	7.05
Mix 2	96.5	0.22	2.27	0.28	0.04	0.01	0.68	0.7	40	3.15	6.85
Mix 3	94	2.5	2.0	0.5	0.2	0.1	0.7	1.0	40	3.05	6.90

The samples were compacted in a hard dye on a hydraulic press at pressure 600 MPa. Sintering occurred in the protective atmosphere within 60 minutes at the temperature of 1120 °C [12]. Compressive strength limits for the samples were checked according to standard ISO 2739:2012 [61].

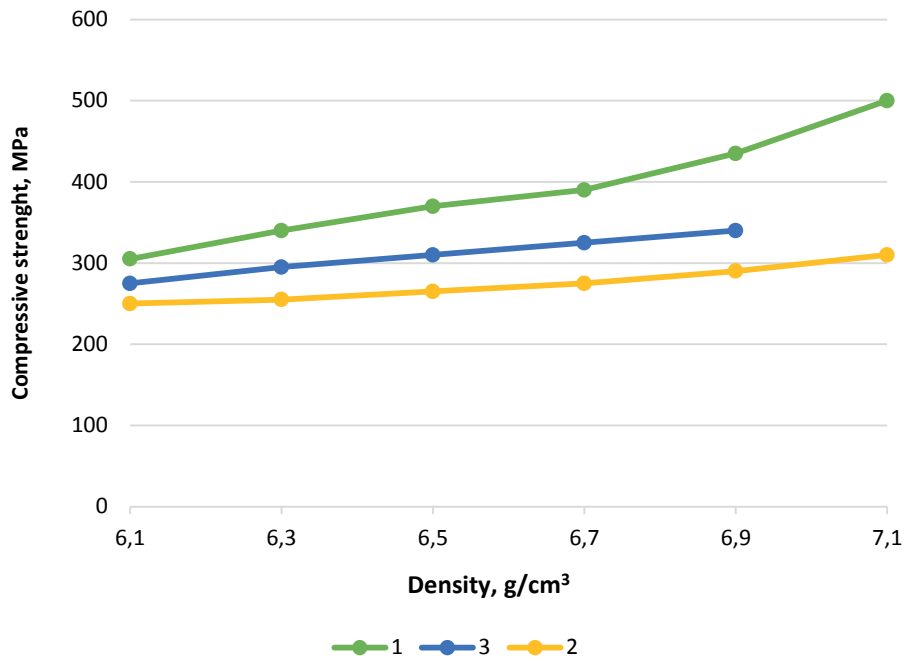


Fig. 2.1. Correlation between compressive strength and material density [12].

The strength of the material from low-alloyed powder in Figure 2.1 (Mix 2) is slightly lower than the one of the control material (Mix 1). Taking into account the significantly lower content of an expensive alloying component in Mix 2, as well as its compliance with the requirements, specified in [31], [54], [55], it could be recommended for manufacturing of metal powder plain friction bearing.

Regression analysis was carried out to forecast the correlation between experimental material density and compressive strength, as well as to study characteristics of the correlation patterns.

Graphical diagram of regression of the low-alloyed powder material (Mix 2) is shown in Figure 2.2.

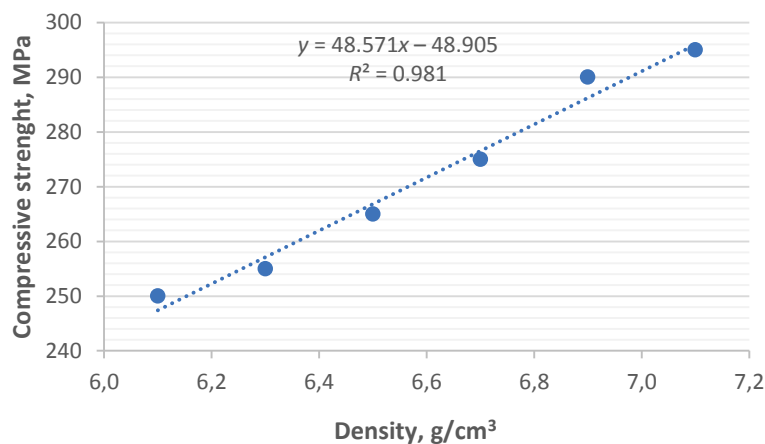


Fig. 2.2. Regression diagram of compressive strength and density for low-alloyed composite material (Mix 2).

The statistical significance of the forecasting model developed by regression and its factors has been evaluated with dispersion analysis method ANOVA (*Analysis of Variance*).

- The calculated value of correlation strength, correlation ratio (R) amounted to 0.99 %.
- The model's accuracy is measured by determination ratio (R^2). According to calculations, $R^2 = 0.981$ or 98.1 %. It means that 98.1 % of material strength variation depends on the material density.

Model-based material strength fluctuations are shown in Figure 2.3.

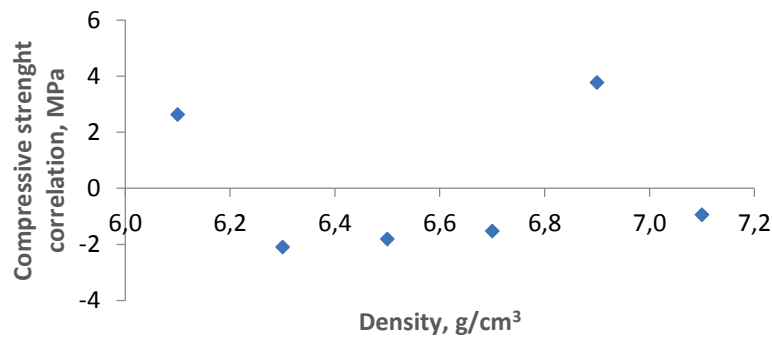


Fig. 2.3. Calculated compressive strength correlation.

Based on the calculation results it may be concluded that the strength of the material under research considering mathematical model-based possible fluctuations corresponds to the requirements of manufacturing metal powder plain friction bearings and use in pivot assemblies of brake lever transmission of railway cars.

In further investigation of low-alloyed composition, a metallographic study has been carried out to determine the microstructure of the material.

For the purpose of microstructural analysis of the low-alloyed material, coarse cuts have been fabricated with the help of metallographic equipment *PRESI* [63]. *Mecatome 255/300* was used for sample cutting; *Mecapress II* – for the coarse cut pressing; *Mecatech 334* – for the coarse cut polishing (Fig. 2.4).



a) *Mecatome 255/300*

b) *Mecapress II*

c) *Mecatech 334*

Fig. 2.4. *PRESI* metallography unit.

An optical microscope *Keyence VHX-2000* (Fig. 2.5) has been used to analyse the microstructure of the material [62].



Fig. 2.5. *Keyence VHX-2000*.

Microstructure of Sample 2 demonstrates evenly distributed porosity (Fig. 2.6).

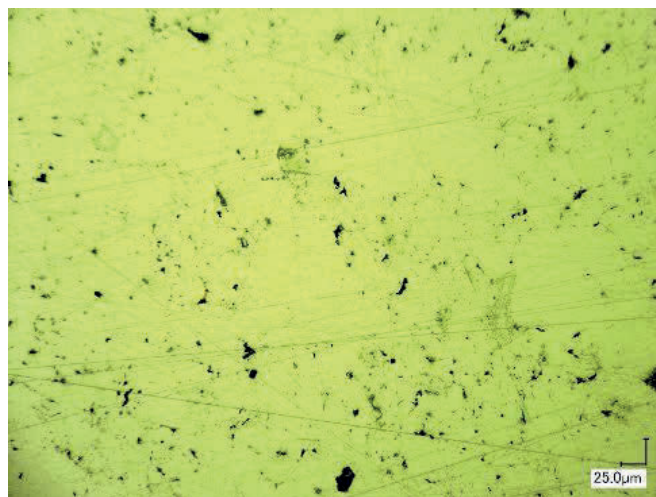


Fig. 2.6. Microstructure of a low-alloyed powder metal material [12].

The research showed that the use of Mixes 1 and 3 in the manufacturing of metal powder plain friction bearings may cause problems in achieving chemically and structurally homogeneous workpieces, as they are produced whilst stirring original powders, but Mix 2 is prepared by atomization of melted steel into the given chemical composition, which is followed by addition of hard lubricant [20]. Therefore, to manufacture metal powder plain friction bearings for brake lever systems, designed for operation under shock impact and in a complex constrained state, it is feasible to use low-alloyed powder composition – Mix 2.

2.1.2. Measurements of Tribological Properties and Surface Quality of Experimental Parts

To assess the surface metrological quality of the low-alloyed bearing and the investigated part thereof, *Taylor Hobson Ltd.* 3D measurement system has been used.

Roughness measurement has been carried out with the help of a profilometer, which allows defining both average profile height Rz , and average arithmetical profile deviation Ra .

Signals from the sensor are transmitted to the electronic unit via the electronic amplifier, which converts the read displacement values and shows them on the display as a measurement result (Fig. 2.7).

2D roughness parameters (Ra ; Rz) have been measured (according to ISO 4287 “Surface texture: Profile method – terms, definitions and surface texture parameters”);

- Ra – average arithmetical profile deviation;
- Rz – profile roughness height parameter (the sum of average absolute deviation for five profile minimum and five profile maximum peaks along the baseline).

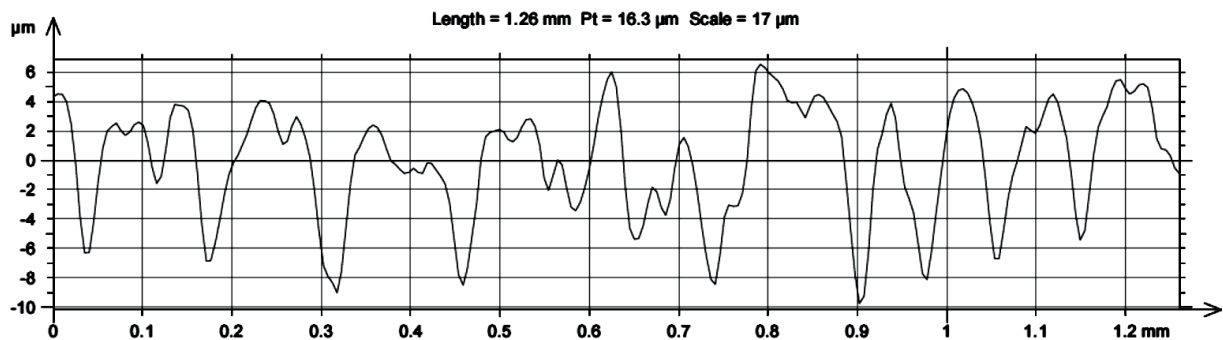


Fig. 2.7. Roughness profile diagram of an experimental part.

Further on, 3D texture parameters have been measured (according to EN ISO 25178-2 “Surface texture: Areal – Part 2: Terms, definitions and surface texture parameters”) [58].

The images of surface of the obtained 3D powder part are shown in Figure 2.8.

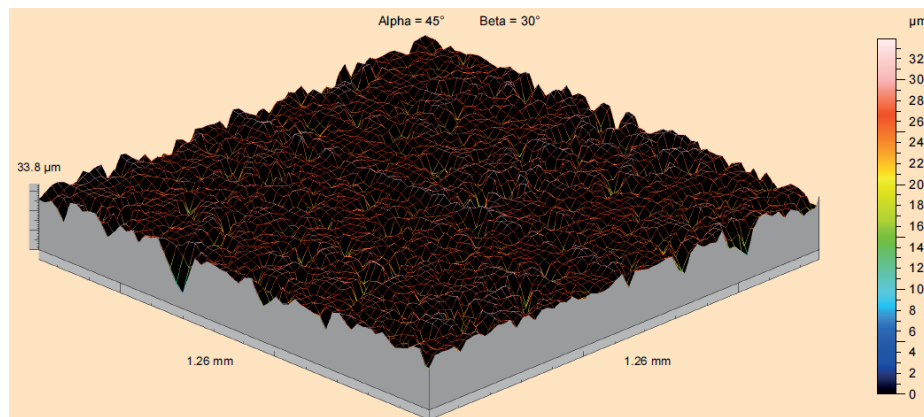


Fig. 2.8. 3D image of low-alloyed powder part surface [20].

The 3D texture parameters of the considered powder parts after the measurements, as well as the 2D measurement results are presented in Table 2.2.

Table 2.2

Roughness and Surface Texture Parameters of the Investigated Low-Alloyed Powder Parts [20]

2D amplitude roughness parameter	$Ra, \mu\text{m}$	2.37
	$Rz, \mu\text{m}$	11.2
3D amplitude texture parameter	$Sa, \mu\text{m}$	2.65
	Ssk	-1.56
3D spatial parameter	Str	0.766
3D functional parameter	$Vmc, \text{mm}^3/\text{mm}^2$	0.0187
3D hybrid parameter	Sfd	2.56

Measurement results confirm that the investigated powder part from the low-alloyed powder material has a comparatively high surface quality. It should be noted that the surface is sufficiently close to isotropic, because the value of Str parameter (surface texture ratio that measures the surface isotropy) is close to 1 (the maximum Str value). The largest value of the functional Vmc parameter (scale-constrained surface material volume that specifies the material area, which forms the surface between different heights) demonstrates good surface load bearing capacity due to the large material volume, which remains in contact under normal operation.

The values of the high hybrid parameter Sfd (close to 3 – the maximum Sfd value) partly confirm the following hypothesis: it is impossible to characterize appropriately the determined-chaotic surface such as a porous powder material surface after compaction and sintering with the help of standard two-dimensional roughness parameters. Thus, it is most likely that the obtained 2D measurements are inaccurate due to complex workpiece surface.

The value of the negative amplitude Ssk parameter (scale-constrained surface asymmetry shows surface height symmetry degree related to the middle plane) confirms the surface capacity to bear the load of the lubricant.

Tribology

Tribological analysis according to DIN 50324 “Tribology; testing of friction and wear model test for sliding friction of solids (ball-on-disc system)”, ASTM G99 “Standard test method for wear testing with a pin-on-disk apparatus”, and ASTM G133 “Standard test method for linear reciprocating Ball-on-flat sliding wear” has been carried out with the help of the *CSM Instruments* tribometer. Friction coefficient as the function of time, revolution (number of rotation cycles), and friction along the length of the road for the investigated part are shown in Figure 2.9.

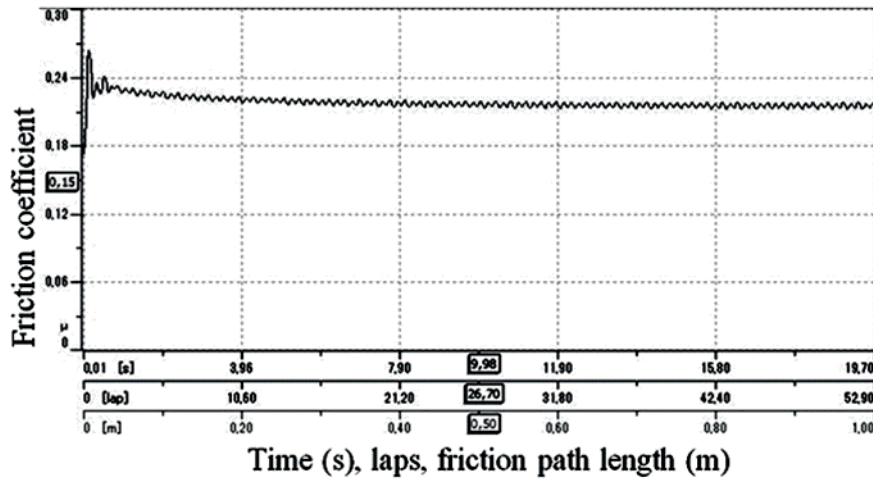


Fig. 2.9. Friction coefficient as the function of time, number of rotation cycles, and friction along the length of the road [20].

A stable friction rate curve is observed with comparatively small fluctuations along the entire friction length. Visual inspection after the tests for traces of wear or surface cold flow demonstrated that during the tests standard friction process was occurring. The average value of friction coefficient for low-alloyed powder bearing amounted to $\mu = 0.22$.

Tribotechnical properties of experimental bearings determined by the test results confirm their conformity for use in brake lever transmission assemblies of railway cars.

2.3. Study of Densification in Pulsed Magnetic Field

Integrated technologies are characterised by the feature that during operation of one source of loading, another one functions at the once set (more often the beginning or the end) moment of the production cycle.

Integrated processes can include vibration-induced shaking and pulsed densification, radial dynamic lengthwise densification of workpieces with their gradual movement, static densification on the hydraulic press, and pulsed densification [14], [17].

The research has been carried out using Hogan AB powders. Data on the materials is presented in Table 2.3.

Table 2.3

Iron-Based Powder Materials

No	Iron powder brand	Production technique	Additional components
1	NC 100.24	Renewed	4 % Cu + 0.6 % K
2	ASC 100.29	Atomized	1.5 % Cu + 0.15 % K
3	SC 100.26	Renewed	2.0 % Cu + 0.15 % K
4	Distaloy AB	Pre-alloyed	Cu (1.5 %), Ni (1.75 %), Mo (0.5 %) 0.15 % K

A hydraulic press with maximum strength of 100 kN was used for densification. A 10 mm diameter steel dye was placed on the press frame. The depth of the charging chamber was 20 mm. The lower punch was equipped with an electrically conductive plate and installed on the flat inductor (Figs. 2.10 and 2.11), and connected to the pulsed current magnetizer *Impulse magnetizer U-series* with the set discharge energy 2.5 kJ (25 000A).

First, the powder was subjected to treatment in a hydraulic press with strength 50 kN, further on – to a single or multiple impulse exposure from the inductor, connected to the pulsed current magnetizer.

The flat copper wire inductor with the cross-section 6 mm² and 12 plies was used. The lower punch 4 mass was 98 g, the copper plate mass – 25 g.

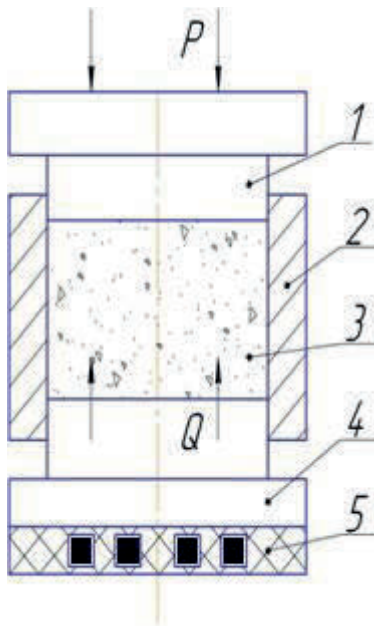


Fig. 2.10. Powder compaction in a hard dye, pulse-magnetic compaction (PMC) hybrid technological layout [18]:

- 1 – punch; 2 – container; 3 – powder;
- 4 – lower punch; 5 – inductor.

Fig. 2.11. Experimental device [18].

Compaction density δ has been evaluated by measuring the punch depth. Test results are presented in Figures 2.12–2.14.

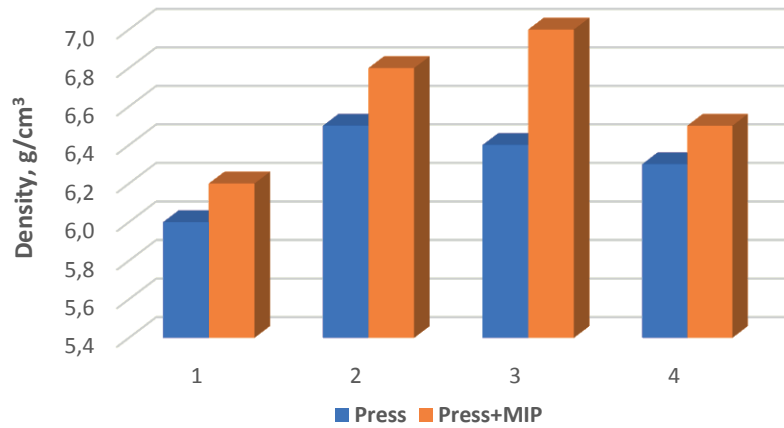


Fig. 2.12. Changes in powder composition (Table 2.3) density during densification [18].

The results (Fig. 2.12) show that exposure to a shock impulse raises the compact density for all powder compositions. The highest density increase is observed at peak levels of the magnetizer discharge energy (Fig. 2.13). Influence of the number of discharge impulses is particularly pronounced, as their number is small. If the number of impulses exceeds 10, this influence becomes less noticeable (Fig. 2.14).

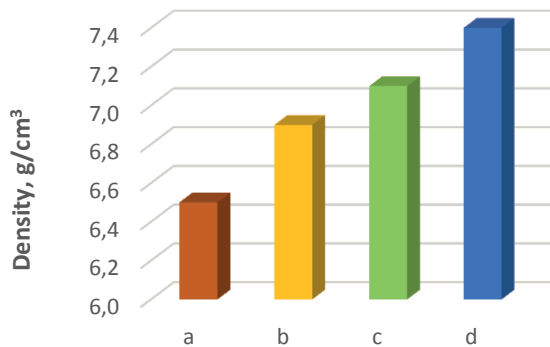


Fig. 2.13. Compact density changes depending on specific discharge energy: a – 0.8 kJ/cm³; b – 0.9 kJ/cm³; c – 1.0 kJ/cm³; d – 1.2 kJ/cm³ [18].

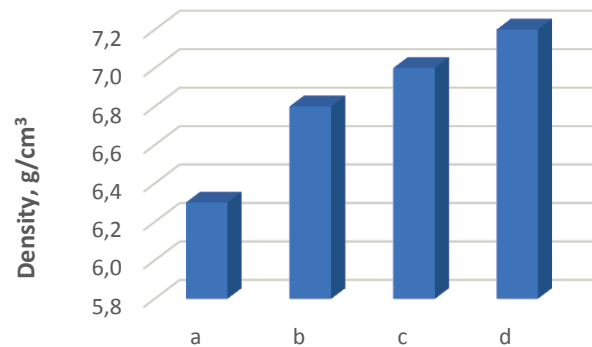


Fig. 2.14. Density changes depending on the number of impulses with specific discharge energy 0.9 kJ/cm³: a – 1; b – 5; c – 10; d – 15 [18].

As demonstrated by experiments, application of integrated densification methods causes growth of powder material density. The most convenient method to be applied for lower height workpieces is powder compaction in hard dies with the help of electromagnetic impulses.

In the case of brake lever bearing manufacturing for railway cars, a certain compaction technique can be recommended for fabrication of experimental samples, for investigation of new sample composition properties, as well as for manufacturing of lengthy antifriction bearings.

3. METAL POWDER PARTS PRODUCTION DEFECTS AND QUALITY CONTROL MEASURES

3.1. Sintering Defects and Defect Reduction Measures

Whilst sintering powder parts, not only defects related to technology but also faults of precedent operations may be revealed: faults of powder and mix production and formation.

For example, if granules have not been sufficiently deformed during densification, inter-grain pores and remaining granule boundaries will cause granule-related defects in a sintered part. Example of the defect is shown in Figure 3.1.

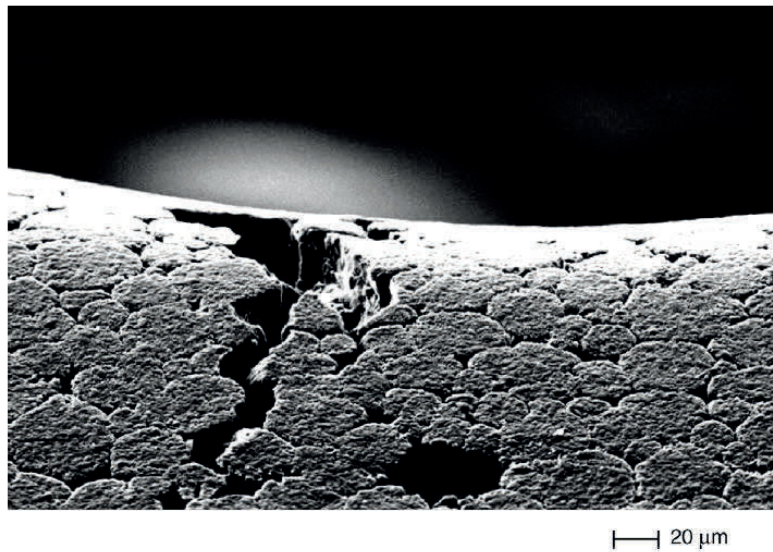
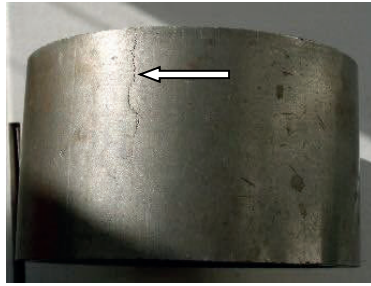


Fig. 3.1. Aggregate grading defects on the surface of metal powder parts [24].

Sintering defects, especially unreparable ones, highly undermine the economic value of PMC parts. When the defect is detected, it is necessary to determine its reasons and take actions for prevention of further defects at all stages of sintering. In addition, it is necessary to develop application of non-destructive control in manufacturing of powder metal parts.

3.2. Ultrasound Quality Control of PM Parts

To determine the degree of homogeneity of metal powder bearings from low-alloyed powder mixes and the opportunity to detect cracks with the help of ultrasound, the TOF technique was applied (time of flight). The aim of the carried-out measurements was to evaluate concurrently heterogeneity of metal powder material properties by the workpiece volume and crack locations. Samples with longitudinal cracks as well as samples without visible defects have been selected for control check (Fig. 3.2).



a



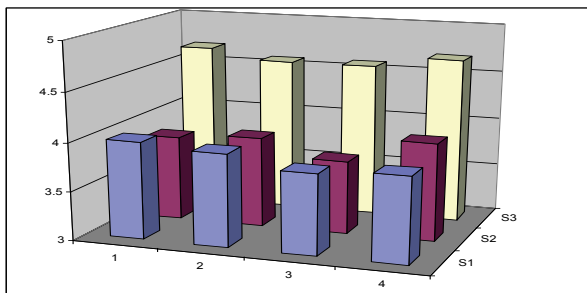
b

Fig. 3.2. Illustration of ultrasound measurements: a) a cracked sample; b) application of adapters [20].

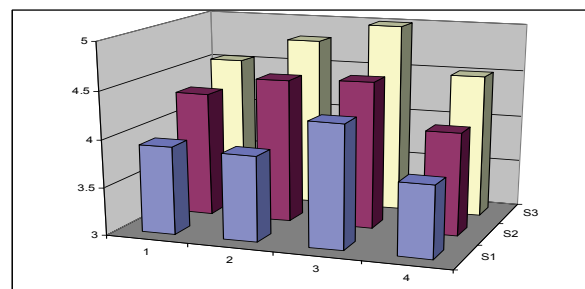
The measurements have been carried out with the help of surface sound scanning at the fixed acoustic base between the emitter and the receiver, equal to 20 mm. The base is oriented perpendicular to the cylinder axis and thus was perpendicular to the crack direction.

Ultrasound signals initiated a 2-period sinusoidal impulse with the carrier frequency of 1 MHz.

Results of speed measurements for ultrasound longitudinal leading wave on a sample surface showed that they are heterogeneous. Sound speed across separate sample zones can vary from 3.75 km/s to 5.00 km/s, which shows that their composition and porosity heterogeneity has been caused by the technological process. Distribution of sound speed across the samples (3.3 a and 3.3 b, respectively) attests a higher property variability along the height than across cross-sectional zones. Sharply increased sound speed was observed in one of the last bands, which is related to specifics of powder densification.



a



b

Fig. 3.3. Distribution of sound speed (km/s) across the perimeter (1–4) and along the height (S1–S3) in two samples [20].

In the area of crack, ultrasound signals were picked up in 10 zones along the workpiece height to evaluate the changes related to the development of the crack. In Figure 3.4 b, two-dimensional images of ultrasound signal array are shown, where the abscissa is ultrasound spread time, the ordinates – signals along the sample height registered row by row, but brightness corresponds to the signal amplitude, the crack height is marked with curved brackets.

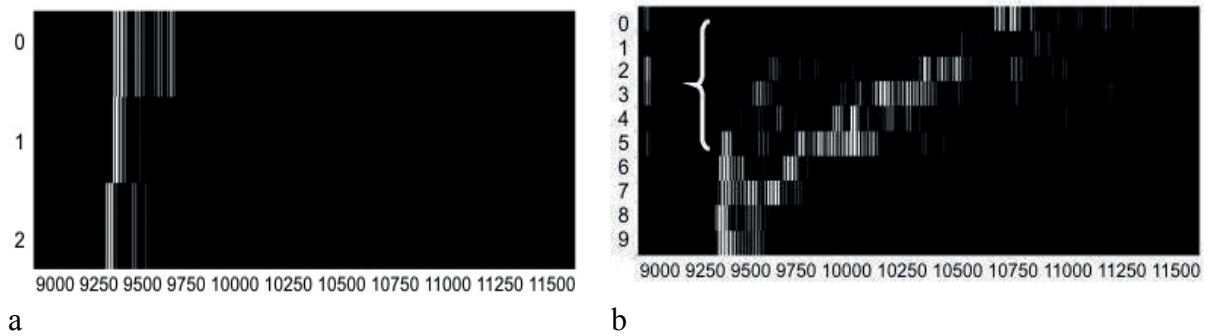


Fig. 3.4. Ultrasound signal image along the height of the samples (in ordinates): a) without defects; b) in the cracked sample [20].

Two-dimensional profile of ultrasound signals precisely shows crack detection upon absence of direct penetration signal and relative strengthening of delayed reflected signals from the opposite end of the workpiece. Thus, signal profiles can serve as crack indicators.

The research showed that ultrasound control (TOF method) allows not only efficient detecting of cracks in PM workpieces, but also is promising when used for material property scattering control by workpiece volume.

3.3. Control of PM Part Connections With the Help of Ultrasound and Radiography

Connection of the investigated parts was carried out using electromagnetic field and a customized inductor [16]. The scheme of the parts connection works and the connected bearings are shown in Figure 3.5.

The research was carried out to assess the quality of antifriction metal powder bearings swaged in pulse magnetic field. Coupled bearings connected in pulse magnetic field are shown in Figure 3.5 b, c. Pressing was made with the help of a 90 mm-high spiral inductor 80 mm in diameter. The inductor was connected to a pulse current baffle. The couples were positioned in the axis zone of the inductor, as shown in Figure 3.5 a. In the applied electromagnetic field, the values of magnetic and electric components on the indicator axis reached 835 A/m and 17 960 V/m.

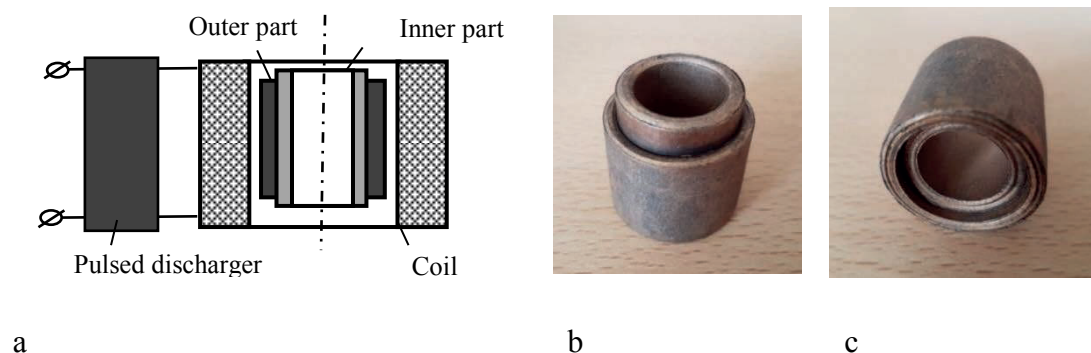


Fig. 3.5. a) principal scheme of powder bushing pressing; b), c) joint bearing-bearing after pressing [33].

Ultrasound defectoscope USM 25 by Krautkramer GE Inspection Technologies GmbH was used for impulse echo testing. A two-element converter Olympus 01JJ4L with working frequency 4 MHz was selected, taking into account specifics of bronze graphite, its porosity, and consequently high signal depletion.

Ultrasound testing

The example of echogram is given in Figure 3.6. In the case of proper adhesion between the connecting parts, the ultrasound wave was able to pass freely through the boundary between the outer and the inner part and be reflected from the inner surface of the wall. Thus, echo reaction was delayed, which corresponds to double wall thickness in both directions. In the case of weak swage and air gap presence between the outer and the inner part, the echo reaction had a two-time shorter delay, which related to full reflection from the wall surface of the outer part. The mean measurement error in the tested samples amounted to 0.14 mm, which indicates high acceptable measurement accuracy [33]. Thus, ultrasound testing confirmed constant connection achieved by pulsed magnetic field swaging and corresponding to ISO standards [59] in ultrasound testing, principal applicability in non-destructive testing.

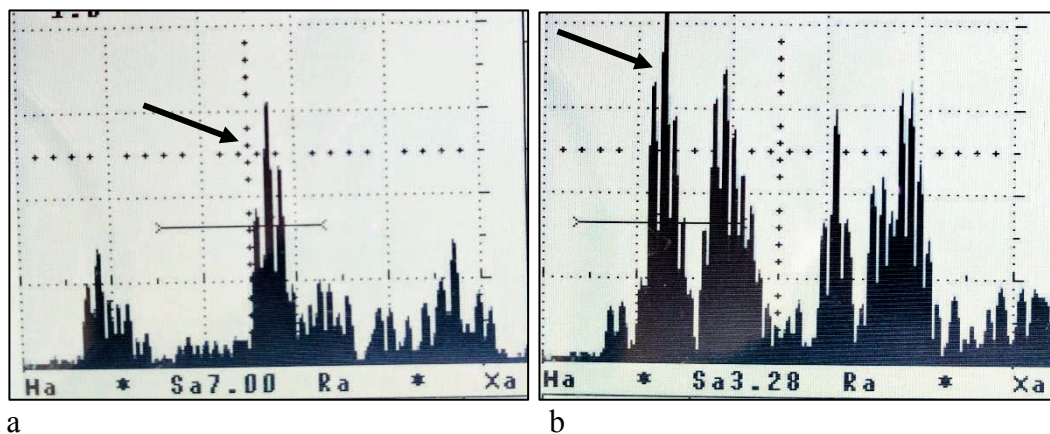


Fig. 3.6. Examples of ultrasound echograms: in the cases of a) tight and b) weak binding. The arrows show reflections that correspond to 7.00 and 3.28 mm thickness [33].

Radiographic control

Mechanical integrity assessment of metal powder parts connection (bearings) after swaging in pulsed magnetic field was carried out using the X-ray apparatus SMART EVO 200D of YXLON.

The apparatus has the focal point 1.0 mm and radiated power with constant potential 750 W, which provides high yields, short exposure time, and high resolution. The principal testing scheme is shown in Figure 3.7.

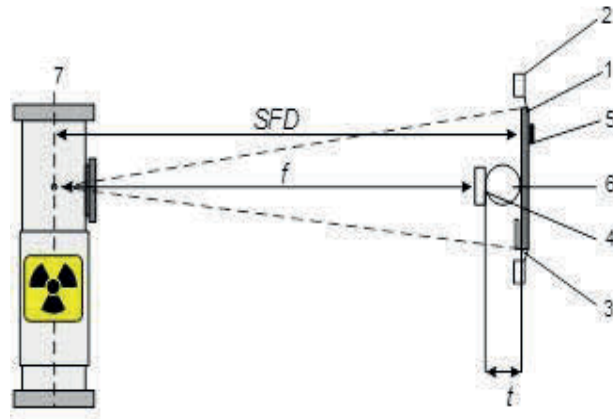


Fig. 3.7. Principal radiographic testing scheme [66]:

1 – lead shield; 2 – film; 3 and 4 – mark of the object and reference point; 5 – indicator of reverse radiation; 6 – object; 7 – x-ray radiation source; f – distance between the source and the object; SFD – distance from the source to the film; t – thickness of the object.

The testing procedure was carried out according to standards LVS EN ISO 17636-1: 2013 [60]. Translucence mode was set on experimental basis using the sample of bearing-bearing connection. Four control irradiations were made with reduction of timing, in this connection, the correlation between the image 7.00 mm and 3.28 mm blackout coefficient and the time of exposure time was discovered, which varied from 4 to 6 times depending on irradiated thickness.

For comparability of results, the approximate relation between the quantity of gamma irradiation for one and the same metal in a monolithic structure and powder structure was defined. Optical thickness of films varied in a range from 2.3 to 3.5.

The films allowed detecting connection defects in the parts of both types. Both circular and axial type gaps between the outer and the inner part were obtained. Figures 3.8 and 3.9 demonstrate comparison of the tight (a) and weak (b) bearing connections from the end and from the side. To obtain the side views and to illuminate better the gaps between the bearings, the images were taken approximately from a 30° angle.

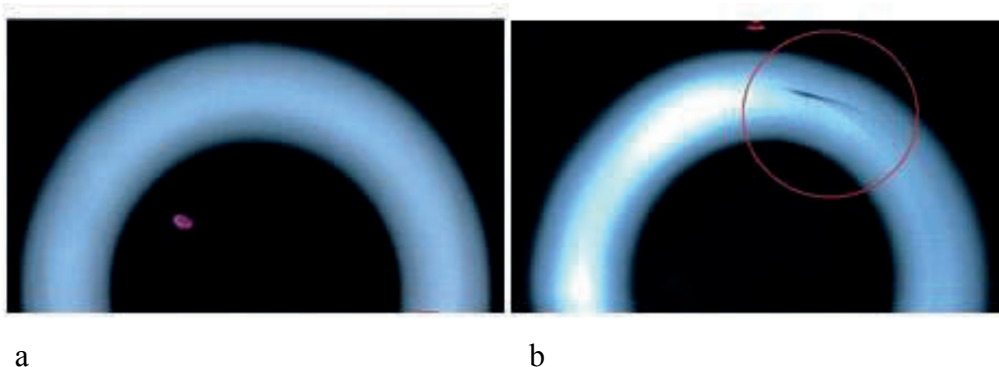


Fig. 3.8. Samples of x-ray films with a) tight and b) weak swage image [33].

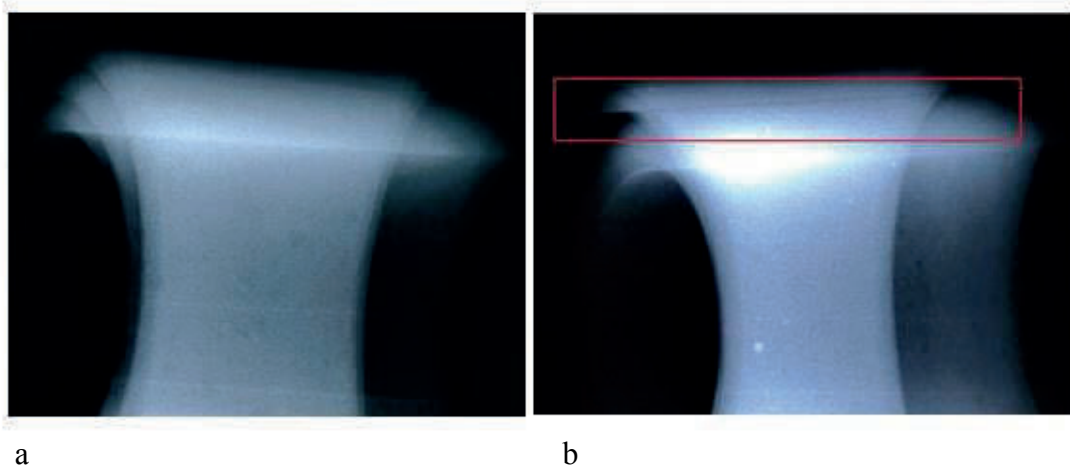


Fig. 3.9. Samples of x-ray films (side view) with a) tight and b) weak swage image [33].

After non-destructive test, the bearings were cut transversely to observe microscopically the boundaries between the inner and outer parts. Samples with tighter and less tight swage, which lead to optically visible gap differences between the inner and outer bearings and vary from zero to many tens of microns, are shown in Figure 3.10. In the case of too tight swage, adhesion between the parts occurs at the level of interfacial microcrystalline penetration, thus providing for mechanical integrity.

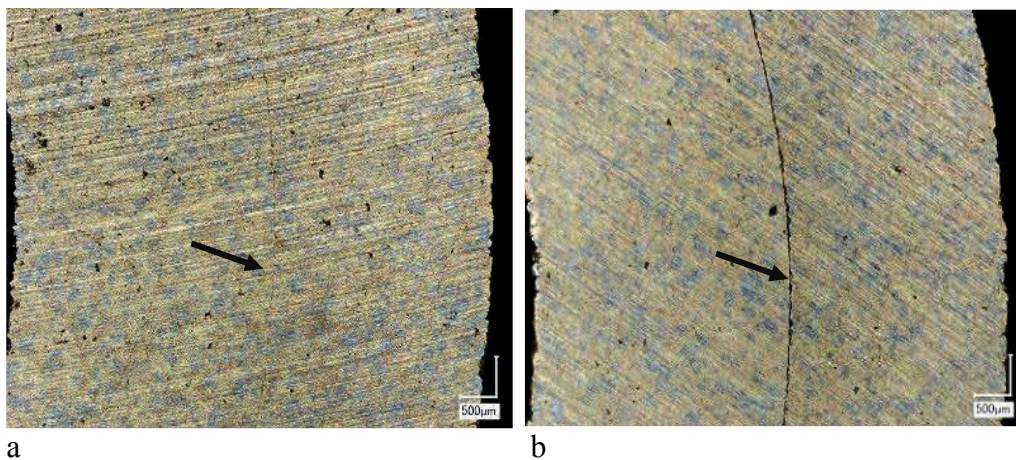


Fig. 3.10. Samples of joint fragments with a) tight and b) weak integrity between the inner and outer bearing; the arrows show the joint boundary [33].

Comparison of approaches

During the tests, both non-destructive testing methods showed similar sensitivity in detection of parts with tight and weak swage. The difference between ultrasound and radiography is based on their physical principles, when ultrasound detected a mechanical crack, which prevented spread of an elastic wave, and x-rays showed an empty space in the material. As for the prospective industrial application, ultrasound is given preference due to a simpler and cost-effective equipment, as well as due to fast operation and data interpretation. Radiographic method is beneficial for contactless testing and visualisation.

Assessment of powder metal antifriction bearing connection quality with the help of non-destructive tests showed sensitivity of both ultrasound and radiographic methods in detection of tight and weak swage. Difficulties in application of standard ultrasound tests for bearing-bearing connection were caused by a greater depletion of ultrasound signals in comparison with powder bronze graphite connection with a cast metal.

Pulse magnetic swage provides for tight connection, which conducts ultrasound unobstructedly and does not generate echo reaction at 4 MHz frequency. Weak connection areas were detected in the same way as early ultrasound echo signals coming from the external wall, they are visible in gap x-ray films. Both methods are promising enough to be implemented in industrial quality control of metal powder part swaging.

4. RESEARCH ON SECONDARY OPERATIONS

4.1. Determination of Optimal Parameters for Mechanical Treatment of Porous Metal Powder Components

Many constructive parts made of powders do not require mechanical treatment (MT), but in a number of cases, particularly in the manufacture of complex parts or with high requirements to the accuracy of dimensions, mechanical treatment is mandatory. Most commonly sintered powder products are subjected to additional treatment by calibrating and cutting. Moreover, achieving final accuracy of dimensions without MT is not always technically and economically expedient [4].

Systematic studies of treatment when cutting sintered powder materials (SPM) have been carried out since the mid 1960s. The studies are reflected in the works of A. Artamonov, I. Armarego, B. Beļkevičs, V. Kononenko, and other authors [2], [6], [45].

The presence of pores in a powder product makes it difficult to cut products, decreases durability of the instruments, despite the fact that generally less cutting force is applied in the treatment of porous products than in the same treatment but without pores. Roughness is often a good indicator of the productivity of a mechanical component, since irregularities on the surface can form a crack or corrosion initial formation centers. As porosity increases, the endurance properties of SPM decrease. This results in a slight improvement of the treatment capacity due to a decrease in the cutting force and, respectively, the temperature during the treatment. However, due to the porosity of waste, the cutting process of SPM takes place with breaks that accelerate the wear of the cutting instrument [28].

Prior to performing experiments in mechanical processing, the nature of the specific cutting forces, contact loads, and tension from the cutting mode and cutting geometry dependencies have been determined. By using the finite element method (FEM), heat flows, fields and temperature on the contact surfaces of the instrument and the surface layer of parts have been considered. Calculations of the stress condition in the surface layer and its porosity have been made.

In the Thesis of Skorikov [51], the following key cutting parameters are recommended for the SPM turning with elevated porosity: cutting rate 150 m/min, feeding 0.1–0.3 mm; cutting depth 0.1–3.0 mm. In addition, it is recommended to select the front angle of the cutter within 25–28° and rear 5–20°.

Studies have been carried out on mechanical treatment of low-alloy metal powder bushings in order to identify the optimal treatment parameters and assess the quality of the treated surface.

The antifriction sliding bushing of the lever braking system of a car, made from material based on Fe-C-Cu, has been as a test part. The bushing is made of powder material containing less than 0.3 % of Ni and Mo and low in phosphorus [20].

Cutting tool

The selected cutting plate is designed for cutting parts from the product groups ISO P (steel) and ISO M (stainless steel). The cutting plate has the following code ISO: VBMT 11 03 04-PF (Fig. 4.1). Metal powder bushings can be viewed as the Group M material and, therefore, the particular cutting plate has been found suitable for the treatment operations.

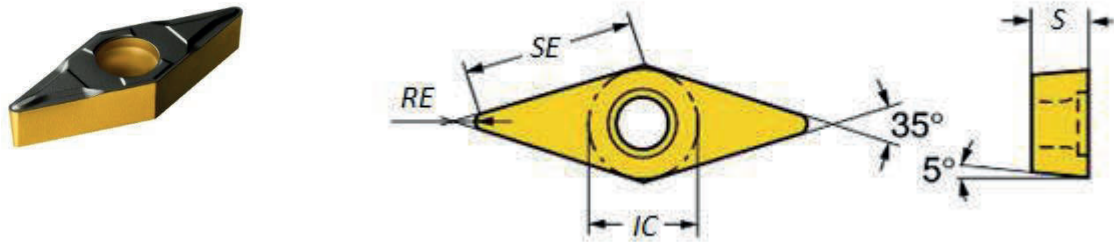


Fig. 4.1. Cutting plate, where RE – tip radius 0.3969 mm; LE – cutting edge length 11.0709 mm; IC – diameter of the drawn circle 6.35 mm; S – plate thickness 3.175 mm, donated by Sandvik Coromant® [21].

Surface roughness parameters

In the process of shaping the parts, roughness appears on their surface – a series of relatively small-size variable projections and cavities.

The first studies on forecasting surface roughness have been conducted only on the basis of geometrical correlations – the geometry of the cutting plate and its movement along the blank. On the basis of geometric correlations, the maximum surface profile roughness Ra_{\max} can be determined using the following Equation [21]:

$$Ra_{\max} = \frac{f^2}{8RE}, \quad (4.1)$$

where f is feeding, mm/rev., and RE is tip radius.

Equation (4.1) can only be used if the cutting depth is less than the RE tip radius. If the tip radius is ignored and the cutting edge angle is taken into account, the maximum roughness of the Ra_{\max} profile is expressed using the following Equation [12]:

$$Ra_{\max} = \frac{f}{4(\text{ctg}\varphi + \text{ctg}\varphi_1)}, \quad (4.2)$$

where φ is main cutting-edge angle, and φ_1 is small cutting-edge angle.

This equation can be used when the cutting depth is larger than the radius of the cutting plate RE and large feeds are used. It was decided to use 3D parameters of the surface roughness as primary parameters and 2D parameters or profile roughness parameters as secondary ones.

Three-dimensional surface roughness parameters are defined in standard ISO 25178. The standard defines many parameters, but the most commonly used parameter is the arithmetic mean surface height Sa (μm), which is determined by the following Equation [21]:

$$Sa = \frac{1}{A} \iint_A Z(x, y) dx dy, \quad (4.3)$$

where A is measurement cross-sectional area, and $Z(x, y)$ is function representing surface height relative to mounting plane or cylinder.

Cutting parameters

Following recommendations of the manufacturer of cutting plates, the following fine treatment operation data have been selected: cutting depth a is 0.5 mm, feeding f is 0.08 mm/rev. and 0.1 mm/rev.; and cutting rate v is 130 m/min and 150 m/min. The cutting and feeding depth has been selected within the range offered, except for the cutting speed. The cutting speed has been selected beyond the range proposed as the cutting will be executed in dry mode – without the use of coolant.

The cutting depth remains constant as it does not provide adaptive features such as cutting speed and feeding. A forecast mathematical model can be developed after the results of the experiment. The next model can be configured to provide adaptive adjustment of feeding and cutting rate during treatment, which provides the required surface roughness adjustments. It is more difficult to achieve adaptive characteristics depending on the cutting depth. Cutting depth is closely related to the tool trajectory that limits adaptive changes during the treatment process.

Turning treatment has been carried out on the *Okuma L200 E-M* lathe. The turning scheme is shown in Figure 4.2 a.

Since the metal powder to be tested is a part with thin walls and deformations exposed during mechanical treatment (Fig. 4.2 b), a special accessory (Fig. 4.2 c) was manufactured to exclude deformation during the turning process.

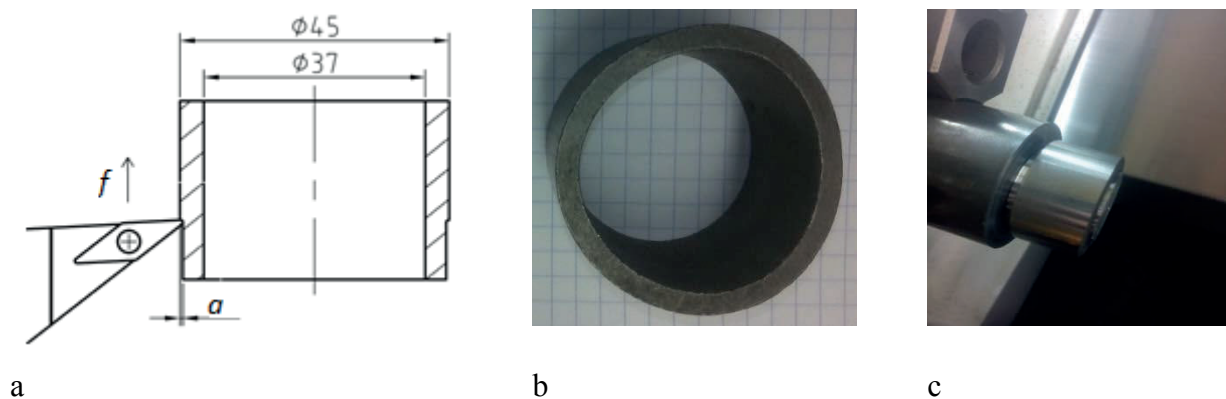


Fig. 4.2. a) bushing treatment scheme; b) bushing deformed at the holder due to high pressure; c) bench for installing bushing by using a special accessory [21].

It is known from theory [2] that out of cutting modes, feeding and cutting rate have the most significant effect on the process of surface roughness formation.

Following the results of the research (Table 4.1), it can be concluded that the best surface roughness can be achieved at the feeding rate of 0.08 mm/rev. and the cutting rate of

130 m/min. In practice, the same result can be achieved by increasing the cutting rate by 20 m/min, thus making it 150 m/min. A different picture will appear if the feeding is changed. When the feeding f was changed by increasing it from 0.08 mm/rev. to 0.1 mm/rev., the surface roughness increased almost twice. It can be concluded that the change in feeding during one revolution f (mm/rev.) affects changes in the surface roughness of the powder parts much more than the cutting rate v .

Table 4.1

Selection of Optimal Parameters of Cutting After Surface Roughness Measurements [21]

Eksperiment No	Average roughness of profile Ra , μm	Average roughness of surface Sa , μm	Average roughness of square surface Sq , μm	Cutting depth a , mm	Feeding f , mm/rev.	Cutting rate v , m/min
1	0.74	1.62	2.73	0.5	0.1	130
2	0.30	0.41	0.54	0.5	0.08	130
3	0.57	0.74	0.91	0.5	0.1	150
4	0.32	0.44	0.68	0.5	0.08	150

The following features have been noticed after the results of the cutting experiments. Surface roughness 3D parameters showed a sharp increase in surface roughness. However, the roughness parameter of the 2D profile did not indicate the next rapid increase. The samples were analysed further and, following a graphic presentation of the roughness of the three-dimensional surface, it was found that the sample of Experiment 1 had far more surface defects than other samples (Fig. 4.3 b).

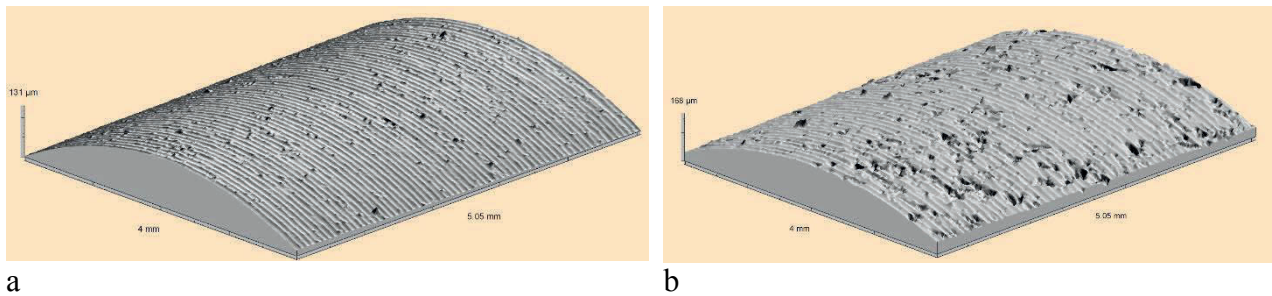


Fig. 4.3. Graphic presentation of the roughness of three-dimensional surface of Experiment No. 2 (Fig. 3 a) and Experiment No. 1 (Fig. 3 b) [21].

This discrepancy is related to the fact that measurement of the roughness of 2D profile (determination of the Ra parameter) is performed in only one row and characterises only this line. Thus, if the defects are not on the measurable line, they are ignored, providing false information about the surface.

In turn, the roughness parameters of the three-dimensional surface include more detailed information about the surface. In this case, the defects were taken into account and the actual surface roughness characteristics were presented. Accordingly, the specific experiment indicates the need for three-dimensional measurement of the surface roughness instead of

two-dimensional measurements. Therefore, the three-dimensional surface roughness parameters should be used in sectors where the quality determines productivity.

The chip form, which is convenient to remove from the work area of technological equipment, is currently an important characteristic of the cutting process. The form and size of chips usually depend on the characteristics of the material to be processed, as well as on the speed of turning of the part and the depth of the cutter feed (Fig. 4.4).

As a result, the chip morphology was studied during the treatment of powder parts.

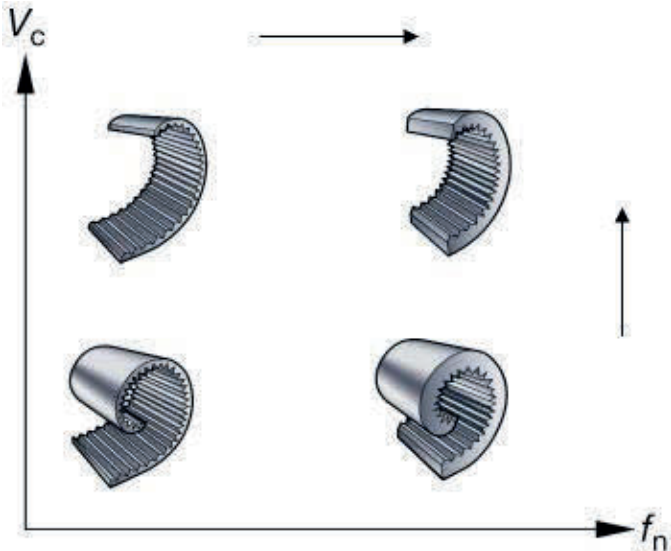


Fig. 4.4. Morphology of chips depending on the speed and feed depth [65].

The chips obtained are classified as discrete or segment chips. These chips are easy to collect, process, and use. Geometric dimensions are shown in Figure 4.6. Following the study and measurement of the chip, it can be concluded that the specific form of chips of the powder-parts treatment process does not cause additional difficulties for the treatment.

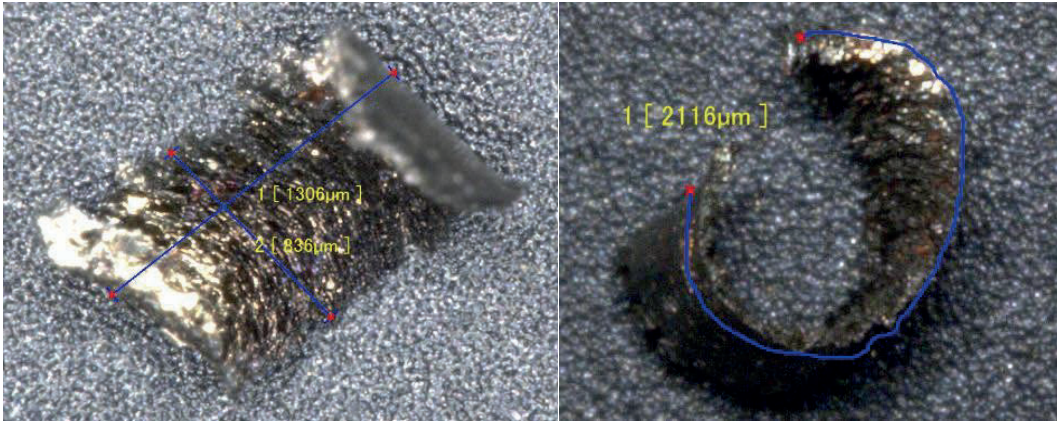


Fig. 4.6. Morphology of chips where a chip segment, 836 µm wide, is shown, the anticipated length is 1306 µm and the total length is 2116 µm [21].

The reserach has been conducted with the aim to examine the effects of cutting parameters on surface roughness parameters, particularly on the roughness parameters of the three-dimensional surface when processing powder parts.

Following the research results, the best surface roughness ($Sa = 0.41 \mu\text{m}$) has been achieved from the assigned range of cutting parameters by using the following modes: cut depth $a = 0.5 \text{ mm}$; feed $e = 0.08 \text{ mm/rev.}$; and cutting rate $v = 130 \text{ m/min}$ [21].

Surface roughness measurements have demonstrated that the roughness parameters of the 3D surface more accurately describe the measured surface than the roughness parameters of the 2D profile, providing more reliable surface data. Measurement of the roughness of the three-dimensional surface for assessing the surface of powder parts after cutting may be recommended as the main measurement method.

The morphology of chips does not indicate that there are any additional problems for removing technological equipment from the work area and has been found as satisfactory throughout the entire range of cutting modes.

4.2. Enhancing the Antifriction Properties of Metal Powder Parts

4.2.1. Impregnating Porous Powder Parts

Interest in reducing friction rates and wear of anti-friction powder boxes is boosted by the global trend and the desire for ecological and economic optimisation in the development of anti-friction materials.

Friction, wear, and lubrication are of major economic importance as these factors determine the service life of machines and equipment [30].

To ensure similar lubrication of friction components and mechanisms, solid lubrication materials are used, which can be classified into the following groups.

1. Inorganic substances:
 - layered (fire-resistant metal dihalides (molybdenum, tungsten, niobium graphite, fluorine graphite, boron nitride, talc, mica, etc.));
 - non-layered (chlorides, fluorides, metal iodides, metal oxides, soft metals Pb, Sn, Cd, Jn, Ga, Ag, Al, and others).
2. Organic polymeric materials:
 - fluorine polymers, polyamides, polyethylene, and others [23], [37].

For practical use, treatment of material in a dispersible environment (oil suspensions) with long-term immersion is most commonly used. This ensures a reduction in roughness and an increase in the stability of the tribological properties of liquid lubricating materials.

4.2.2. Disperse Medium and Disperse Components

The behaviour of oil lubricants in operation depends mainly on their chemical composition and work conditions (temperature, pressure, oxygen action, etc.).

I. Korogodskis, by looking at disperse particles of wear (during application), conditionally divided them into two groups:

Group 1 – large-size solid particles (above 5μ) to be removed from lubricating oil;

Group 2 – crushed soft particles and small particles, which must remain in oil as they have a positive effect.

The extent of effects of the second group of disperse particles on tear and wear of friction pairs depends on their concentration in oil. According to I. Korogodskis, their optimal concentration is 2.5 % [38].

Disperse components of graphite and molybdenum disulphide particles introduced in oil lubricants are most widely used. Graphite has very high chemical stability and it is practically inert to radioactive radiation [7], [13].

The presence of porosity in powder parts contributes to the intensification of diffusion; the element to be introduced into the materials is distributed in depth by grains and inter-grain borders, while diffusion in porous powder materials takes place across the entire surface of the particles, as illustrated schematically in Figure 4.7 [42].

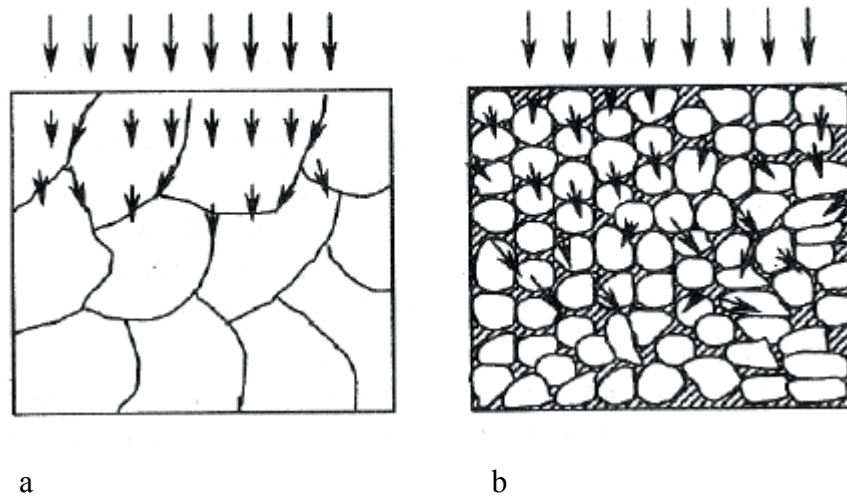


Fig. 4.7. Impregnation scheme: a) without pores; b) porous powder material.

Selection of oil and dispersion components

For experimental studies, MS-20 oil has been selected as a dispersion medium. Stability against oxidation of MS-20 oil during storage is maintained by a significant number of natural inhibitors, which cannot be deactivated with a small amount of oxygen dissolved in oil. This characteristic contributes to increased purity of experimental studies in different directions.

When small dispersion particles appear in lubricating oils (further referred to as “dispersive phase”), dispersive systems are formed viscosity of which differs from that of disperse medium (oil).

Inorganic layered solid lubricant materials (MoS_2 , MoSe_2 , WS_2 , WSe_2 , etc.) maintain operating properties in a wide range of temperatures between $-100\text{ }^\circ\text{C}$ and $+1000\text{ }^\circ\text{C}$, capable of withstanding extreme contact pressures comparable to high-strength steel flowability limits, are stable in vacuum, aggressive and inert environments. The adhesion of dihalcogenides to the surface of metals is such that a slight contact pressure (0.4–0.5 MPa) is sufficient with a relative offset to connect the lubricant particles to the surface when forming a common film [39].

4.2.3. Friction Coefficient Reduction Studies

For the reduction of the friction factor, studies have been conducted on impregnation of sintered porous metal powder parts (sliding bushings) with nanoparticles. The studies have been carried out on bushings used in the vehicle brake lever system and made from the powder mixture AHC100.29 + 2.27 % Cu + 0.22 % Ni + C [20].

MS-20 oil has been used as disperse medium and tungsten dihalcogenide powders – disulphide WS_2 and diselenide WSe_2 as disperse additives.

The microstructure and appearance of the bushings are shown in Figure 4.8.

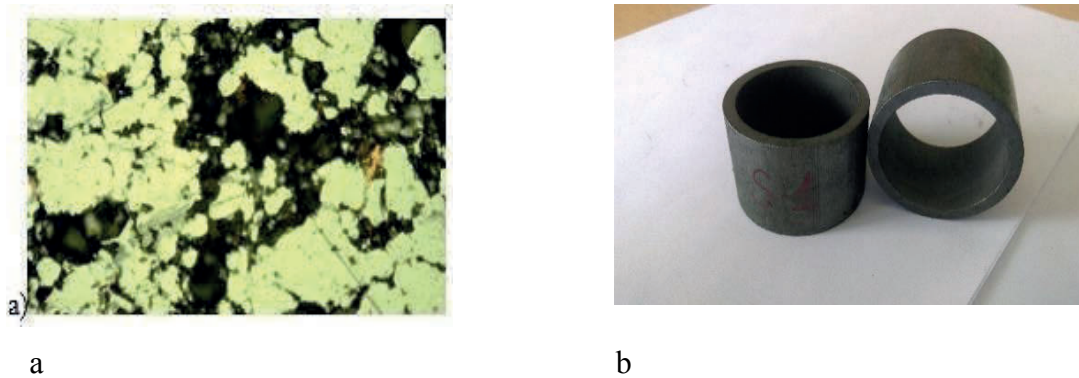


Fig. 4.8. a) microstructure and b) appearance of the bushings [32].

In the course of the research, the bushings were impregnated with MS-20 oil, as well as the same oil with 4 % tungsten disulphide nanoparticle additives – WS_2 , and 4 % tungsten diselenide additives – WSe_2 .

Tungsten disulphide nanoparticles have a spherical shape with a diameter of 30–50 nm (Fig. 4.9 a), whereas tungsten diselenide particles have a flat shape with a mean size of 5 nm \times 70 nm as shown in Figure 4.19 b [34], [35].

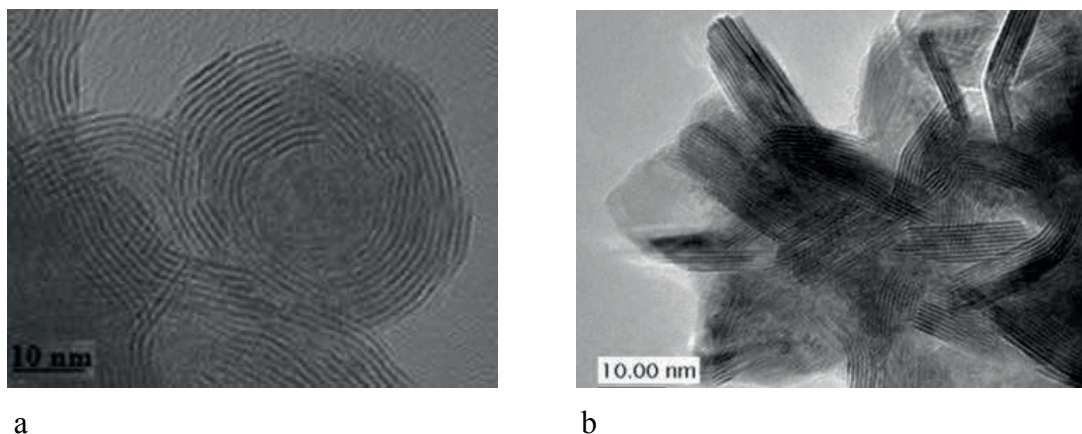


Fig. 4.9. TEM micrography with a) WS_2 and b) WSe_2 nanoparticles [32].

Tribological testing of samples impregnated with oil MS-20, MS-20 + 4 % WS_2 , MS20 + 4 has been carried out in friction conditions in pairs with bearing steel at a load of 210 N and a rotation rate of 200 rpm.

Trials have been conducted using a friction machine PBD-40. In addition, tests in the extended temperature range have been carried out on the equipment for assessing the tribological properties of materials (LV Patent No. 15225) [27], [49].

The samples have been exposed to contact with a normal load of 210 N. Then the process of rotation of the working valve with the cylindrical sample was started at a rotation frequency of 200 rpm. One test time lasted 1000 s.

Time-dependent rotation friction moment for MS-20 impregnated with oil and lubrication compositions is shown in Figure 4.10. In all cases, deformation occurs during second two of the experiment, a friction moment being equal to 0.12–0.1 nm for all lubrication compositions. The identity of friction moments and time intervals until deformation may be related to the identity of the initial conditions of friction expressed, firstly, in a pore division with a certain thickness of oxide film.

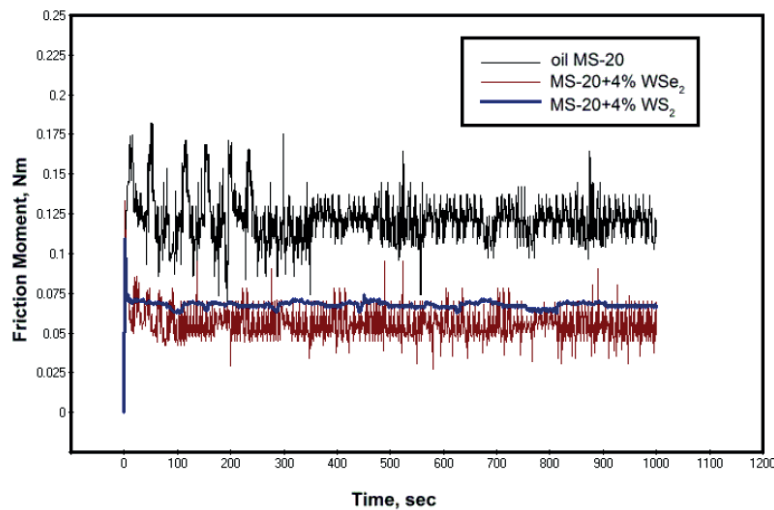


Fig. 4.10. Dependence of friction moment on time when testing samples impregnated with MS-20 oil and lubrication compositions contain 4 % WSe₂ and 4 % WS₂ [32].

The graph in Figure 4.10 shows that the friction moment dependency on time, the bushings impregnated with MS-20 oil, and the lubrication composition with WSe₂ are “jumps” in a friction moment that may be associated with disintegration of contact and oxide films. Later, when the lubricating oil is removed from the pores, the variation in torque is reduced.

On average, the friction moment was equal to ≈ 0.056 N·m and ca. ≈ 0.067 N·m for oils modified with tungsten disulphide and diselenide nanoparticles respectively [32].

The most stable friction moment was demonstrated by bushings impregnated with lubrication composition MS-20 + 4 % WS₂. It can be noted that the “leaps” inherent in the onset of friction with the decomposition of the oxide film, which contains spherical nanoparticles of tungsten disulphide (WS₂), do not appear. It may be, on the one hand, due to a small thickness of oxide film and, on the other, due to the spread of the lubrication composition, which has been pushed into a local section along the surface of the oxide film, which has not yet materialised but entered into contact. In this case, the spherical form of the particles to be entered may contribute to more stable antifricition indicators.

CONCLUSIONS

Based on the experimental studies within the framework of the Doctoral Thesis and the obtained results, the author has provided a comprehensive description of the technological process, as well as the compression parameters and the sintering of powder parts required for the manufacture of experimental prototypes. Based on the studies with experimental parts, advantages of the low-alloyed powder on an iron basis (Fe-C-Cu with an alloying element content of 0.22 % Ni and 0.28 % Mo) have been demonstrated for the manufacture of bushings of the brake lever mechanism of a car.

Following the results of non-destructive tests, testing characteristics of the sintered porous powder materials have been identified. When testing the quality of metal powder parts with ultrasound, the test results have demonstrated the ability of this method to detect cracks and inaccuracies of powder parts. The radiographic research, together with an ultrasound method, accurately determines the quality of the bushing connection.

The Doctoral Thesis has set the prospects for using static, dynamic, and hybrid methods of pressing powder parts by using an electromagnetic field.

According to the results of the cutting experiments with porous powder parts, optimal modes have been established to ensure even roughness of the surface of the part to be processed. It has been concluded that changes in the feeding rate affect changes in the roughness of the surface of powder parts more significantly than the cutting rate.

Following the results of studies on experimental bushings impregnated with lubrication composition MS-20 + 4 % WSe₂ and MS-20 + 4 % WS₂, the average friction moment decreases by ≈53 % and ≈44 %, respectively, compared with oils impregnated with MS-20 without the input particles.

The research has shown that the spherical form of tungsten disulphide particles contributes to more sustainable antifriction indicators and provides more stable operation of friction components, practically bypassing the friction pairing stage, which is not a minor factor when applying the respective technology to antifriction bushings of the rolling stock braking system.

The following tasks of the Doctoral Thesis have been completed:

1. Manufacturing technology for metal powder parts has been studied as well as technological parameters for pressing and sintering, the characteristics of the powder and the effects of alloying elements on the strength and safety of the parts to be manufactured.
2. Criteria have been set for using metal powder materials in railway transport.
3. Studies have been conducted with experimental parts demonstrating the suitability of a mixture of low-alloy powders based on Fe-C-Cu with a low content of alloying elements for use in the manufacture of antifriction sliding bushings for the braking lever of rolling stock.

4. Prospects for the hybrid extrusion method of metal powder components have been demonstrated and the extrusion parameters by using the electromagnetic field have been defined.
5. Specific features and non-destructive tests have been set for suitability of ultrasound and radiographic techniques to be used in the quality control of porous metal powder parts.
6. Mechanical treatment studies have been performed for porous metal powder sliding bushings and a mechanical processing methodology for these parts has been developed based on the roughness of the part treated.
7. Based on experiments performed within the framework of the Doctoral Thesis, a method has been proposed for impregnating antifriction metal powder parts with WS₂ and WSe₂ nanoparticles containing oil emulsions, reducing the coefficient of friction and enhancing the tribotechnic properties.

BIBLIOGRAPHY OF THE SUMMARY

1. Ahlström, M., Thyssen, J., Menne, T., Johansen, J. Prevalence of nickel allergy in Europe following the EU Nickel Directive – a review. 2017, *Contact Dermatitis*. vol. 77, pp. 193–200. Available from: doi: 10.1111/cod.12846.
2. Armarego, E. J. A., Shi, G., Verezub, S. Modeling the Basic Cutting Action and Machining Performance of Sintered Metallic Materials. *Machining Science and Technology*, 2001. vol. 5 no. 3, pp. 353–373. Available from: doi: <https://doi.org/10.1081/MST-100108620>
3. Beiss, P. Principles of Metal Powder Compaction. In: *European Powder Metallurgy Association Training Course*, Germany, Aachen, Sept, 2005, pp.109–134.
4. Blais, C. Machining of PM Materials: A Secondary Shaping Operation of Primary concern. 2008, *International Journal of Powder Metallurgy*. vol. 44, no. 2. pp. 13–14.
5. Chasoglou, D., *Surface Chemical Characteristics of Chromium-alloyed Steel Powder and the Role of Process Parameters during Sintering*. PhD Thesis. Chalmers University of Technology: 2012. 90 p.
6. Christopher P. Adams, Carl Blais, and Deepak S. Madan. *Machining & Machinability of PM Components*, Report by Metal Powder Industries Federation. Metal Powder Industries Federation: 2006.
7. Dresel, W., Mang, T. (ed.). *Lubricants and Lubrication, vol. 2. 3rd Edition*. Weinheim: Wiley-VCH Verlag GmbH & Co. KGaA, 2017. 1262 p. ISBN 978-3-527-32670-9
8. European Powder Metallurgy Association (EPMA). *Introduction to Powder Metallurgy: The Process and its Products*. 2008, Shrewsbury, U.K.,
9. German, R. M. *Powder Metallurgy & Particulate Materials Processing*. Princeton NJ USA: Metal Powder Industries Federation, 2005. 522 p. ISBN 0-9762057-1-8.
10. Glass, S. J. and Ewsuk, K. G. (1997) Compaction science and technology. *MRS Bull.*, 22 (12), 24–28.]
11. Karas, L., Flodin, A. Wear Investigation of Porous Material Impregnated with Oil and Nanoparticles. in: *Euro PM2017 Proceedings: New Frontiers in PM Steels*. Milan: EPMA, 2017.
12. Kirby, E. D., Zhang, Z., Chen, J. C. Development of an accelerometer-based surface roughness prediction system in turning operations using multiple regression techniques, in: *Journal of Industrial Technology*, 2004, vol. 20, no. 4, pp. 1–8.
13. Klamann, D. *Lubricant and related products*, Weinheim: Wiley-VCH, 1984. 489.p. ISBN 978-3527260225
14. Lapkovskis, V., Mironovs, V., Zemčenkovs, V., Boiko, I. Processing of Powder Materials by Pulse Electromagnetic Field. In: *Proceedings of 11th World Powder Metallurgy Congress (PM2010)*, Italy, Florence, 10–14 October 2010. Shrewsbury: European Powder Metallurgy Association, 2010, pp. 519–524. ISBN 9781899072101.
15. Lewandowski, J., Seifi, M. Metal Additive Manufacturing: A Review of Mechanical Properties. *Annual Review of Materials Research*. 2016, vol. 46. pp. 151–186. Available from: doi: 10.1146/annurev-matsci-070115-032024

16. Mironovs, V., Gluschenkov, V., Belyaeva, I., Tatarinovs, A. Combined Methods of Pulsed Magnetic Compaction of Metal Powders. In: *World PM 2016 Congress and Exhibition Guide*, Germany, Hamburg, 9–13 October, 2016. Hamburg: 2016, pp. 56–56.
17. Mironovs, V., Korjakins, A., Tatarinovs, A., Barone, E., Gluschenkov, V. Combined Static-Dynamic Compaction of Metal Powder and Ceramic Materials. IOP Conference Series: Materials Science and Engineering, 2017, vol. 251: *3rd International Conference on Innovative Materials, Structures and Technologies (IMST 2017)*, pp. 1–7. ISSN 1757-8981. e-ISSN 1757-899X. Available from: doi:10.1088/1757-899X/251/1/012020
18. Mironovs, V., Stankevich, P., Beljaeva, I., Glushenkov, V. Static-Dynamic Powder Material Compaction Methods. In: *15th International Scientific Conference, Engineering for Rural Development. Latvia, Jelgava, 25–27 May 2016*. vol. 5, Jelgava: Latvia University of Agriculture, 2016, pp. 1128–1132. ISSN 1691-5976
19. Mironovs, V., Stankevich, P., Eiduks, J. Tendencies in the Field of Application of Metal-Powder Materials for Repair and Maintenance of Railway Equipment. *Procedia Computer Science*, 2019, vol. 149, pp. 344–348. ISSN 1877-0509. Available from: doi:10.1016/j.procs.2019.01.146.
20. Mironovs, V., Stankevich, P., Tatarinov, A., Zemchenkov, V., et al. Mechanical and Acoustical Properties of Bushings Made of Low-Alloyed Materials and Used in Brake Systems of Transport Vehicles. *Materials Science and Engineering*, 2015, vol. 96, no. 1, pp. 1–9. ISSN 1757-8981. e-ISSN 1757-899X. Available from: doi:10.1088/1757-899X/96/1/012016
21. Mironovs, V., Stankevics, P., Kromanis, A., Lungevics, J. Influence of Machining Parameters on 3D Surface Roughness of Powder Bushings. *Key Engineering Materials*, 2017, vol. 721, pp. 378–382. ISSN 1013-9826. e-ISSN 1662-9795. Available from: doi:10.4028/www.scientific.net/KEM.721.378.
22. Morl, L., Heinrich, S., Peglow, M. Fluidized bed spray granulation. *Handbook of Powder Technology*, 2007, vol. 11, pp. 21–188. Available from: doi: https://doi.org/10.1016/S0167-3785(07)80037-6
23. Muson, B. R., Okiishi, T. H., Huebsch, W. W., Rothmayer, A. P. *Fundamentals of Fluid Mechanics*. 7th.ed. New York: John Wiley & Sons, Inc., 2012. 747 p. ISBN 978-1-118-11613-5.
24. Oberacker, R. Powder compaction by dry pressing. In: Riedel, R., Chen, I.-W. (eds.). *Ceramics Science and Technology*, 2011. vol. 3, pp. 1–37. ISBN: 978-3-527-31157-6.
25. PM Industry Roadmap Technology Update for the Powder Metallurgy Industry. METAL POWDER INDUSTRIES FEDERATION, 105 College Road East, Princeton, New Jersey. ISBN 08540-6692, 2017. 24 p.
26. Rahaman., M. N. (2003) *Ceramic Processing and Sintering*, 2nd edn, Marcel Dekker, New York, Basel.
27. Rīgas Tehniska Universitāte. *Iekārta materiālu triboloģisko īpašību novērtēšanai*. Viktors Mironovs, Pāvels Stankēvičs, Jānis Rudzītis, Int. Cl.:G01N3/56. Iesniegšanas datējums 2016-12-29. Patenti un Preču Zīmes. LV15225. 2017.12.20.

28. Robert-Perron. E., Blais. C. Green Machining: Parametrs, Applications, And Sintered Properies. 2008, *International Journal of Powder Metallurgy*. vol. 44, no. 2. pp. 41–53.
29. Schatt, W., Wieters, K. P., Kieback, B. *Pulvermetallurgie: Technologien und Werkstoffe*. 2nd ed. Düsseldorf: Springer-VDI-Verlag, 2007. 552 p. ISBN 978-3-540-23652-8.
30. Shi, Z., Jian, P., Xue, P., Chen, D. 2012 The Friction and Wear Characteristic of Iron-based Powder metallurgy materials in Scroll Compressor In Pros. of 21st Int. Compressor Engineering Conference at Purdue. West Lafayette, Indiana, USA, pp. 6–12.
31. Slotwinski, J., Cooke, A., Moylan, S. Mechanical Properties Testing for Metal Parts Made via Additive Manufacturing: A Review of the State of the Art of Mechanical Property Testing. 2015, NISTIR 7847.
32. Stankevich, P., Mironovs, V., Vasilyeva, E., Breki, A., Tolochko, O. The Possibility of Modifying the Elements of the Bearing Assembly with Nanoparticles in Order to Reduce the Friction Coefficient. IOP Conference Series: Materials Science and Engineering, 2017, vol. 251, pp. 1–5. ISSN 1757-8981. e-ISSN 1757-899X. Available from: doi:10.1088/1757-899X/251/1/012084
33. Tatarinovs, A., Mironovs, V., Rybak, D., Stankevich, P. Non-Destructive Testing of Joints of Antifriction Parts Crimped by Pulsed Magnetic Deformation. *Solid State Phenomena*. 2017, Vol. 267, pp. 248–252. ISSN 1662-9779. Available from: doi:10.4028/www.scientific.net/SSP.267.248.
34. Vasilyeva, E., Nasibulin, A., Maximov, M. A., Tolochko, O., et al. Synthesis of Tungsten Diselenide Nanoparticles by Chemical Vapor Condensation Method. *Materials Science* 2015, vol. 21, no. 3, pp. 339–342. Available from: doi: 10.5755/j01.ms.21.3.7356.
35. Vasilyeva, E., Nasibulin, A., Tolochko, O., Rudskoy, A., et al. Application of WSe₂; Nanoparticles Synthesized by Chemical Vapor Condensation Method for Li-Ion Battery Anodes. *Zeitschrift fur Physikalische Chemie* 2015, vol. 229, no. 9, pp. 1429–1437. Available from: doi: 10.1515/zpch-2015-0573.
36. Анциферов, В. Н., Акименко, В. Б., Гревнов, Л.М. Порошковые легированные стали. – М.: Металлургия, 1991. – 318 с.
37. Бирюков, В. П. *Смазочные материалы, топлива и технические жидкости*. М.: МИИТ. 2008. 183 с. ISBN 978-5-7876-0023-0
38. Бреки, А. Д., Васильева, Е. С., Толочко, О. В., Стариков, Н. Е. *Триботехнические характеристики жидких смазочных и полиимидных композиционных материалов, содержащих антифрикционные наночастицы дихалькогенидов вольфрама*. Тула: Изд-во ТулГУ, 2015. 276 с. ISBN: 978-5-7679-3203-0
39. Бреки, А. Д., Кудрявцев, В. В., Диденко, А. Л., Васильева, Е. С., и др. *Триботехнические свойства композиционных покрытий с полиимидными матрицами и наполнителями из наночастиц дихалькогенидов вольфрама для узлов трения машин*. Тула: Изд-во ТулГУ, 2015. 128 с. ISBN 978-5-7679-3113-2.
40. Галай, Э. И., Галай, Е. Э. *Тормозные системы железнодорожного транспорта. Конструкция тормозного оборудования*. Гомель: БелГУТ, М-вообразования Респ. Беларусь, Белорус. гос.ун-трансп. 2010. 315 с. ISBN978-985-468-687-5
41. Гегузин, Я. Е. *Физика спекания*. 2-е изд., перераб. и доп. М.: Наука., 1984. 312 с.

42. Гиршов, В. Л., Котов, С. А., Цеменко, В.Н. *Современные технологии в порошковой металлургии*. Санкт-Петербург.: Изд-во Политехн. Ун-та, 2010. 385 с.
43. Гропянов, А. В., Теплухин, Г. Н. *Материаловедение*. СПб: СПбГУПТД 2017. 78 с.
44. Гропянов, А. В., Ситов, Н. Н., Жукова, М. Н. *Порошковые материалы*. Санкт-Петербург: СПбГУПТД, 2017. 74 с.
45. Дьячкова, Л. Н., Керженцева, Л. Ф., Маркова, Л. В. Порошковые материалы на основе железа.. – Минск.: Тонпик, 2004. 228 с.
46. Карпычев, Владимир Александрович. *Разработка метода системного анализа автотормоза грузового подвижного состава*. Диссертация на соиск. уч. ст. д-ра техн. наук. Москва: [МИИТ], 2000. 157 с.
47. Крылов, В. И., Крылов, В. В., Ефремов, В. Н. *Тормозное оборудование железнодорожного подвижного состава*. М.: Транспорт, 1989. 487 с.
48. Либенсон, Г. А., Лопатин, В. Ю., Комарницкий, Г.В. Процессы порошковой металлургии. Т. 2. Формование и спекание. М.: МИСИС, 2002. 320 с.
49. Миронов, В., Станкевич, П., Дортыньш, В. Машина трения с вертикальной осью вращения. В: Порошковая металлургия: Новые материалы и технологии: порошковая металлургия, композиционные материалы, защитные покрытия, сварка: материалы 13-й Международной научно-технической конференции. Минск, Беларусь. 16–18 Мая, 2018. Беларуская навука, 2018, 351–354 с. ISBN 978-985-08-1838-6.
50. Полюшкин, Н.Г. *Основы теории трения, износа и смазки*. Красноярск: Краснояр. гос. аграр. ун-т. 2013. 192 с. ББК 40.72-082я73.
51. Скориков, А. В. *Теоретические предпосылки обеспечения заданного качества порошковых изделий и рекомендации по их практической реализации*. Автореф. Дисс. д.т.н., 2003. 186 с.
52. Хренов, О. В., Афанасьев Л. Н., Лешок, А. В. Материалы и технология порошковой металлургии. Минск. Белорусский национальный технический университет. 2010. 37 с.
53. Научно-исследовательский институт импульсных процессов с опытным производством: [tiešsaiste]. *Производство изделий с низким коэффициентом трения для нужд машиностроения. [skatīts 2019.g. 20.apr.]*. Pieejams: http://russian.impulse.by/?page_id=356
54. Fine Sinter Co., Ltd. Powder Metallurgy Products, [online]. *Railroad application*. [viewed 21 April 2019]. Available from: <http://www.finesinter.com/english/products/pmp/railway/>
55. *Полувагон модели 12-132-03*. [tiešsaiste]. Руководство по эксплуатации. [skatīts 2019. g. 20. apr.]. Pieejams: <https://ldzcargo.ldz.lv/sites/cargo.ldz.lv/files/%D0%9F%D0%BE%D0%BB%D1%83%D0%B2%D0%B0%D0%B3%D0%BE%D0%BD%2012-132-03.pdf>
56. Abbott Furnace Company. [online]. [viewed 11 April 2019]. Available from: <https://www.abbottfurnaceco.com/sintering-fundamentals>

57. Höganäs iron and steel powders for sintered components, Handbook 1. 2002. [online]. [viewed 2 May 2015]. Available from: https://www.hoganas.com/globalassets/download-media/sharepoint/handbooks--all-documents/handbook-1-material_and_powder_properties_december_2013_0674hog-interactive.pdf
58. International Organization for Standardization. *Geometrical product specifications (GPS) – Surface texture: Areal - Part 2: Terms, definitions and surface texture parameters* [online]. ISO 25178-2:2012 [viewed 4 February 2019]. Available from: <https://www.iso.org/standard/42785.html>
59. International Organization for Standardization. *Non-destructive testing - Ultrasonic testing - Sensitivity and range setting*. [online]. ISO 16811:2012. [viewed 15 February 2019]. Available from: <https://www.iso.org/standard/57782.html>
60. International Organization for Standardization. *Non-destructive testing of welds - Radiographic testing - Part 1: X- and gamma-ray techniques with film*. [online]. ISO 17636-1:2013. [viewed 15 February 2019]. Available from: <https://www.iso.org/standard/52981.html>
61. International Organization for Standardization. *Sintered metal bushings - Determination of radial crushing strength* [online]. ISO 2739:2012 [viewed 1 April 2019]. Available from: <https://www.iso.org/standard/53346.html>
62. Keyence corporation. *Digital Microscope VHX-2000 series* [online]. [viewed 26 January 2019]. Available from: <https://www.keyence.com/products/microscope/digital-microscope/vhx-2000/index.jsp>
63. Presi Metallography. [online]. [viewed 6 January 2019]. Available from: <https://www.presi.com/en/>
64. *Production of Sintered Components*, in Höganäs Handbook 2., [online]. Höganäs AB: 2013. 162p. [viewed 11 April 2019]. Available from: https://www.hoganas.com/globalassets/download-media/sharepoint/handbooks---all-documents/handbook-2_production_of_sintered_components_december_2013_0675hog_interactive.pdf
65. Sandvik coromant. [online]. Metal cutting knowledge [viewed 10 February 2016]. Available from: <https://www.sandvik.coromant.com/en-gb/knowledge/pages/default.aspx>
66. Yxlon Product Catalog. Portable and mobile X-ray systems. [online]. [viewed 5 February 2018]. Available from: https://www.yxlon-portables.com/YxlonPortables/media/pdf/product_catalog/YXLON_Product_Catalog_v1.pdf